AGU ADVANCING EARTH AND SPACE SCIENCE

Biomarker Distributions in (Sub)-Arctic Surface Sediments and Their Potential for Sea Ice Reconstructions

Henriette M. Kolling[1,2] (ID), Ruediger Stein[1,3] (ID), Kirsten Fahl[1] (ID), Henrik Sadatzki[4,5] (ID), Anne de Vernal[6] (ID), and Xiaotong Xiao[7] (ID)

[1]Alfred Wegener Institute, Helmholtz Centre for Polar and Marine Research, Bremerhaven, Germany, [2]Institute of Geosciences, Christian-Albrechts-Universität zu Kiel, Kiel, Germany, [3]MARUM-Center for Marine Environmental Sciences and Faculty of Geosciences, University of Bremen, Bremen, Germany, [4]Department of Earth Science and Bjerknes Centre for Climate Research, University of Bergen, Bergen, Norway, [5]Research School of Earth Sciences, Australian National University, Canberra, ACT, Australia, [6]Centre de recherche en géochemie et géodynamique (Geotop), Université du Québec à Montréal, Montréal, Québec, Canada, [7]Institute of Marine Organic Geochemistry, Ocean University of China, Qingdao, China

Abstract To evaluate the present sea ice changes in a longer-term perspective, the knowledge of sea ice variability on preindustrial and geological time scales is essential. For the interpretation of proxy reconstructions it is necessary to understand the recent signals of different sea ice proxies from various regions. We present 260 new sediment surface samples collected in the (sub-)Arctic Oceans that were analyzed for specific sea ice (IP$_{25}$) and open-water phytoplankton biomarkers (brassicasterol, dinosterol, and highly branched isoprenoid [HBI] III). This new biomarker data set was combined with 615 previously published biomarker surface samples into a pan-Arctic database. The resulting pan-Arctic biomarker and sea ice index (PIP$_{25}$) database shows a spatial distribution correlating well with the diverse modern sea ice concentrations. We find correlations of P$_B$IP$_{25}$, P$_D$IP$_{25}$, and P$_{III}$IP$_{25}$ with spring and autumn sea ice concentrations. Similar correlations with modern sea ice concentrations are observed in Baffin Bay. However, the correlations of the PIP$_{25}$ indices with modern sea ice concentrations differ in Fram Strait from those of the (sub-)Arctic data set, which is likely caused by region-specific differences in sea ice variability, nutrient availability, and other environmental conditions. The extended (sea ice) biomarker database strengthens the validity of biomarker sea ice reconstructions in different Arctic regions and shows how different sea ice proxies combined may resolve specific seasonal sea ice conditions.

1. Introduction

Sea ice plays a crucial role in the Earth's energy budget via the sea ice-albedo feedback (Thomas & Dieckmann, 2010; Wohlfahrt et al., 2004). Further, it restricts heat and moisture exchange between ocean and atmosphere, whereas its formation and melt control the thermohaline properties of the upper water column through brine formation in winter and release of freshwater in summer (Petrich & Eicken, 2010; Thomas, 2012). Hence, the seasonal and longer-term variability of Arctic sea ice is an important component of the global climate system.

Satellite observations illustrate the reduction in Arctic sea ice extent over four decades (e.g., Comiso et al., 2008; Notz & Stroeve, 2018; Perovich et al., 2009; Stroeve et al., 2007, 2012; Stroeve & Notz, 2018), which has raised the concern about the fate of Arctic sea ice. The influence of anthropogenic greenhouse gas emissions and associated atmospheric warming on the recent sea ice loss is very likely (e.g., Notz & Stroeve, 2016), and disentangling the effects of both anthropogenic and natural forcing is a matter of current research (Swart, 2017). Reliable satellite observations are only available since 1978 (Comiso et al., 1997; Parkinson, 2008) and do not adequately represent the full range of sea ice variability. Reconstructions of sea ice cover on time scales beyond satellite measurements are necessary to understand longer-term sea ice changes and their driving mechanisms under various climate forcings. For such reconstructions, specific biogenic and sedimentary proxies preserved in marine sediments (de Vernal, Gersonde, et al., 2013, and references therein) have been used to gather information about past sea ice conditions. These include ice-rafted debris (e.g., Andrews, 2009; Spielhagen et al., 2004; Stein et al., 1994; Vogt et al., 2001) and

assemblages of microfossils, such as foraminifera (e.g., Aagaard-Sørensen et al., 2010; Seidenkrantz, 2013; Werner et al., 2011), ostracods (e.g., Cronin et al., 2010), diatoms (e.g., Koç et al., 1993; Krawczyk et al., 2017; Miettinen et al., 2015), and organic-walled dinoflagellate cysts (e.g., Bonnet et al., 2010; de Vernal, Eynaud, et al., 2005; de Vernal, Rochon, et al., 2013; de Vernal et al., 2001; Pieńkowski et al., 2017; Ribeiro et al., 2012). However, most of these proxies are indirectly related to sea ice (de Vernal, Gersonde, et al., 2013), and preservation can be a problem in Arctic and sub-Arctic settings (Armand & Leventer, 2010; Wollenburg et al., 2001, 2004). The application of sedimentary ancient DNA, which may be a new step toward the determination of the organisms behind different proxies, is yet under development (De Schepper et al., 2019). While a range of proxies enable to gather information on past environmental changes, including sea ice, the ability to semiquantitatively reconstruct paleo sea ice distributions has been significantly improved by a biomarker approach based on the determination of a highly branched isoprenoid (HBI) with 25 carbons (C_{25} HBI monoene $= IP_{25}$) (Belt et al., 2007). This biomarker is exclusively biosynthesized by few diatom species living in Arctic sea ice (Brown et al., 2014; Limoges et al., 2018) (see section 2 for more detailed information). The sea ice proxy IP_{25} appears to be a specific, sensitive, and stable proxy for Arctic sea ice in marine sediments reaching back to Miocene and Pliocene/Pleistocene times (Belt et al., 2007; Knies et al., 2014; Stein et al., 2016; Stein & Fahl, 2013). By combining IP_{25} and specific open-water phytoplankton biomarkers, that is, brassicasterol, dinosterol, and HBI III (Z-isomere), that result in the so called "PIP_{25} index," even more semiquantitative estimates of sea ice concentrations might be possible (Belt et al., 2015; Müller et al., 2011; Smik et al., 2016; for further details see section 2). Studies of the distribution of IP_{25} in surface sediments in several areas provide a good spatial coverage and illustrate the relationship with satellite-observed sea ice conditions at regional scales (Méheust et al., 2013; Müller et al., 2011; Navarro-Rodriguez et al., 2013; Ribeiro et al., 2017; Smik et al., 2016; Wegner Koch et al., 2020; Xiao et al., 2013, 2015). However, only two studies focused on the IP_{25} and PIP_{25} distribution on an Arctic-wide scale (Stoynova et al., 2013; Xiao et al., 2015). Subsequent to these studies, new advances, such as the use of HBI III (Z-isomere) as phytoplankton marker, were made (e.g., Belt et al., 2015, 2019; Köseoğlu et al., 2018; Stein et al., 2017) and opened new options for biomarker-based paleo sea ice reconstructions. Despite the extensive work done in this field, the relationship of different biomarkers to different ecological settings and their use and reliability for sea ice reconstructions is still under debate, especially in an Arctic-wide context. For a full state-of-the-art overview of the IP_{25}/PIP_{25} approach see Belt et al. (2018, 2019).

The main objectives of this study are as follows:

1. to investigate the distribution of specific biomarkers and the applicability of the PIP_{25} approach in surface sediments from Baffin Bay and Fram Strait on 260 new surface sediment samples,
2. to combine the new data with 615 published surface sediment biomarker/sea ice index records into a comprehensive data set ($n = 875$, Table 1; supporting information Table S2) and compare them to satellite-based sea ice concentrations to contribute to a better understanding of biomarker distributions as a basis for sea ice reconstructions on a (sub-)Arctic scale, and
3. to compare the comprehensive sea ice estimates of the new (sub-)Arctic biomarker surface sediment data set with reconstructions based on the application of the modern analog technique (MAT) of Northern Hemisphere dinoflagellate cysts (de Vernal, Rochon, et al., 2013). Thereby to contribute to the overall goal to improve the understanding of sea ice proxy signals and the quality of sea ice reconstructions from sedimentary records.

The final outcome of this study will set a basis for quantitative reconstruction of sea ice parameters, notably seasonal sea ice concentration, based on biomarkers and microfossil assemblages (cf. de Vernal, Rochon, et al., 2013; Matthiessen et al., 2018).

2. Background

Information on marine and terrigenous organic matter input can be derived from specific biomarkers including n-alkanes, sterols, and alkenones, as inferred from studies of modern sediments and paleoenvironmental reconstructions (e.g., Fahl & Stein, 1997, 1999; Meyers, 1997; Stein & Macdonald, 2004). In marine organic matter, brassicasterol and dinosterol have been associated with a wide range of algal groups such as diatoms and dinoflagellates (e.g., Goad & Withers, 1982; Kanazwa et al., 1971; Volkman et al., 1993) and have been often used as open-water phytoplankton biomarker proxies (e.g., Fahl & Stein, 2012; Hoff

Table 1
Summary of Study Areas of New and Published Sea Ice Biomarker Surface Sediment Records Used for the Comprehensive Data Set of This Study

Region	n	Study	Storage	Sample interval	Extraction	Method
Arctic Ocean	21	This study	>4°C/−20°C, glass vial	0–1 cm	US	open column, GC-MS
	65	Xiao et al. (2013)	N/A	N/A	ASE	open column, GC-MS
	78	Xiao et al. (2015)	−30°C	0–1 cm	ASE	open column, GC-MS
	149	Wegner Koch et al. (2020)	−20°C	N/A	saponification	open column, GC-MS
Barents Sea	24	This study	>4°C/−20°C, glass vial	0–1 cm	US	open column, GC-MS
	94	Navarro-Rodriguez et al. (2013)	−20°C	0–1 cm	US	open column, GC-MS
	8	Müller et al. (2011)	−30°C, glass vial	0–1 cm	ASE	open column, GC-MS
	28	Smik et al. (2016)	−20°C	0–1 cm	US	open column, GC-MS
	11	Xiao et al. (2015)	−30°C	0–1 cm	ASE	open column, GC-MS
	101	Belt et al. (2015)	−20°C	0–1 cm	US	open column, GC-MS
Fram Strait and East Greenland Shelf	76	This study	>4°C/−20°C, glass vial	0–1 cm	US	open column, GC-MS
	36	Müller et al. (2011)	−30°C, glass vial	0–1 cm	ASE	open column, GC-MS
	13	Ribeiro et al. (2017)	−80°C	0–0.5/0–1 cm	US	open column, GC-MS
	7	Xiao et al. (2015)	−30°C	0–1 cm	ASE	open column, GC-MS
Baffin Bay (including Hudson Strait and Gulf of St. Lawrence)	139	This study	>4°C/−20°C, glass vial/ plastic bags	0–1 cm/0–2 cm	US	open column, GC-MS
Canadian Arctic Archipelago	15	Belt et al. (2007)	−20°C	N/A	saponification	GC-MS
	14	Belt et al. (2013)	>4°C	N/A	saponification	GC-MS
	2	Pieńkowski et al. (2017)	freeze-dried immediately, stored cold and dark	N/A	US	open column, GC-MS
Bering Sea	39	Méheust et al. (2013)	−30°C, glass vials	0–1 cm	ASE	open column, GC-MS
	22	Wegner Koch et al. (2020)	−20°C	N/A	Saponification	open column, GC-MS

Note. Abbreviations as follows: *n*: number of samples, US: sonication, ASE: accelerated solvent extractor, and GC-MS: gas chromatograph-mass spectrometer.

et al., 2016; Knies et al., 2017; Müller et al., 2009; Volkman, 1986; Volkman et al., 1993). In this context, it must be noted that brassicasterol may be synthesized also by lacustrine algae and transported by rivers into the ocean as described, for example, in studies from the Kara and Laptev Seas (Fahl et al., 2003; Fahl & Stein, 1999; Hörner et al., 2016). To a minor extent, brassicasterol might be produced by sea ice diatoms as postulated by Belt et al. (2013, 2018). Thus, brassicasterol should be interpreted cautiously and ideally in combination with other biomarkers.

For sea ice reconstructions, a sea ice diatom-derived HBI IP$_{25}$ has been established as a reliable proxy for the presence of seasonal spring sea ice in the Arctic and sub-Arctic (Belt et al., 2007; Brown et al., 2014; for reviews see Belt, 2018, 2019; Belt & Müller, 2013; Stein et al., 2012). It has been used to reconstruct sea ice conditions back to Pliocene and Miocene times (Knies et al., 2014; Stein et al., 2016; Stein & Fahl, 2013).

For semiquantitative sea ice reconstructions, Müller et al. (2009, 2011) have combined the IP$_{25}$ sea ice proxy with open-water phytoplankton biomarkers, notably brassicasterol (P$_B$IP$_{25}$) and dinosterol (P$_D$IP$_{25}$), in the so-called "PIP$_{25}$ index" calculated after the following equation:

$$PIP_{25} = IP_{25}/(IP_{25} + (\text{phytoplankton biomarker} \times c))$$

The balance factor *c* is the ratio of mean IP$_{25}$ concentration and mean sterol concentration, counterbalancing generally higher concentrations of sterols compared to IP$_{25}$. Xiao et al. (2015) were the first to combine a large data set of biomarker surface samples from the (sub-)Arctic regions. They found higher correlations with sea ice concentrations for P$_B$IP$_{25}$ and P$_D$IP$_{25}$ indices for a (sub-)Arctic wide *c* factor compared to regional *c* factors. The *c* factor is considered as a major uncertainty of the PIP$_{25}$ approach (e.g., Belt, 2018; Belt & Müller, 2013), which will be addressed further in section 6.

Despite these uncertainties, previous studies showed that modern surface sediment biomarker concentrations and P$_B$IP$_{25}$ and P$_D$IP$_{25}$ indices reflect modern satellite-based sea ice conditions relatively well on the East Greenland Shelf and in Fram Strait (Müller et al., 2011), the Barents Sea (Navarro-Rodriguez et al., 2013) and the central Arctic Ocean (Xiao et al., 2015).

Smik et al. (2016) have further developed the PIP_{25} approach by introducing a triunsaturated HBI alkene (HBI III, $C_{25:3}$, and Z-isomere). HBI III (Z) is produced by marine diatoms of the genera Pleurosigma and Rhizosolenia (Belt et al., 2017; Rowland et al., 2001) and seems to show a more direct association with marginal ice zone (MIZ) productivity than the open-water phytoplankton biomarkers brassicasterol and dinosterol. Hence, environmental reconstructions may benefit from the application of HBI III (Z), as it appears to be produced by a smaller group of organisms than brassicasterol and dinosterol and has been suggested to display a higher ecological sensitivity to sea ice (Belt et al., 2015). Furthermore, HBI III (Z) and IP_{25} showed similar concentrations in some of the studied regions, which made the use of the balance factor c unnecessary in the calculation of the $P_{III}IP_{25}$ index (Belt et al., 2015; Smik et al., 2016). So far, the use of HBI III (Z) has only been tested in surface sediments from the Barents Sea, the Norwegian Sea region (Belt et al., 2015; Köseoğlu et al., 2018; Smik et al., 2016; Smik & Belt, 2017), and an East Greenland fjord system (Ribeiro et al., 2017). The application of the $P_{III}IP_{25}$ index and the requirement of the c factor for its calculation have yet to be investigated in other regions.

Recently, Belt et al. (2019) determined the distribution pattern of two diatom-derived triunsaturated HBI lipids (Z-isomere and E-isomere) in surface sediments from the Barents Sea and found an association between the relative proportion of these two HBIs (i.e., the "HBI TR_{25}" ratio) and satellite-derived spring chlorophyll a concentration. Based on these findings, the HBI TR_{25} ratio has been proposed as a potential proxy for the spring phytoplankton bloom. A wider spatial distribution of this approach is needed to verify its circum-Arctic applicability.

Following Belt et al. (2019), we calculated the TR_{25} index as follows:

$$HBI\ TR_{25} = [C_{25}\ HBI\ III\ (Z)]/[C_{25}\ HBI\ III\ (Z) + C_{25}\ HBI\ III\ (E)]$$

Another sea ice-related compound seems to be the diunsaturated HBI alkene (here termed HBI II), which has been identified in Arctic and Antarctic sediments (Belt et al., 2007; Lamping et al., 2020; Massé et al., 2011; Vare et al., 2009; Vorrath et al., 2019). In the Southern Ocean, HBI II is produced by sea ice/landfast ice-dwelling diatoms and has been successfully used as a proxy for landfast ice termed $IPSO_{25}$ (Belt et al., 2016). The origin and potential as an environmental proxy of HBI II in the Northern Hemisphere are still under discussion. Possible links to sea ice or sea surface temperature (SST) (by the ratio of IP_{25} and HBI II, termed DIP_{25} index) have been proposed for specific regions (e.g., Cabedo-Sanz et al., 2013; Fahl & Stein, 2012; Müller & Stein, 2014; Vare et al., 2009; Xiao et al., 2013) According to Belt et al. (2018), however, the latter seems to be more unlikely given the near-uniform temperatures found at the base of seasonal sea ice where IP_{25} and HBI II are biosynthesized. Based on the often-observed coproduction of IP_{25} and HBI II, Belt et al. (2018) postulate that HBI II might represent an even "better" sea ice proxy than IP_{25} or at least a useful substitute in cases where IP_{25} is absent (or below its detection limit) (cf. Andrews et al., 2018). Nonetheless, a consistent signal for the Northern Hemisphere has not yet been demonstrated.

3. Regional Setting

The Arctic Ocean and sub-Arctic seas are highly influenced by the seasonal expansion and retreat of sea ice. Only the central Arctic Ocean is permanently covered by multiyear sea ice, several meters thick, whereas the adjacent shelf seas are covered by seasonal sea ice, between a few cm to 2 m thick (Figure 1; Cavalieri et al., 1996, updated 2017). Sea ice is transported through the Arctic Ocean and also exported by the Beaufort Gyre and via the Transpolar Drift (Figure 1).

The majority of Arctic sea ice export (860×10^3 km^2/a; Zamani et al., 2019) occurs via western Fram Strait by the East Greenland Current (EGC), which flows south along the East Greenland coast and carries large amounts of Arctic water masses and sea ice into the North Atlantic (Figure 1; Aagaard & Coachman, 1968a, 1968b). Sea ice formation starts on the shallow shelves of the Arctic Ocean. Both sea ice formation and export reach a maximum in March (Michel et al., 2015) when sea ice extends as far south as Iceland.

Fram Strait is influenced by the export of cold Arctic water masses and sea ice in the west and inflowing warm Atlantic water masses in the east. In eastern Fram Strait, sea ice conditions are less severe due to
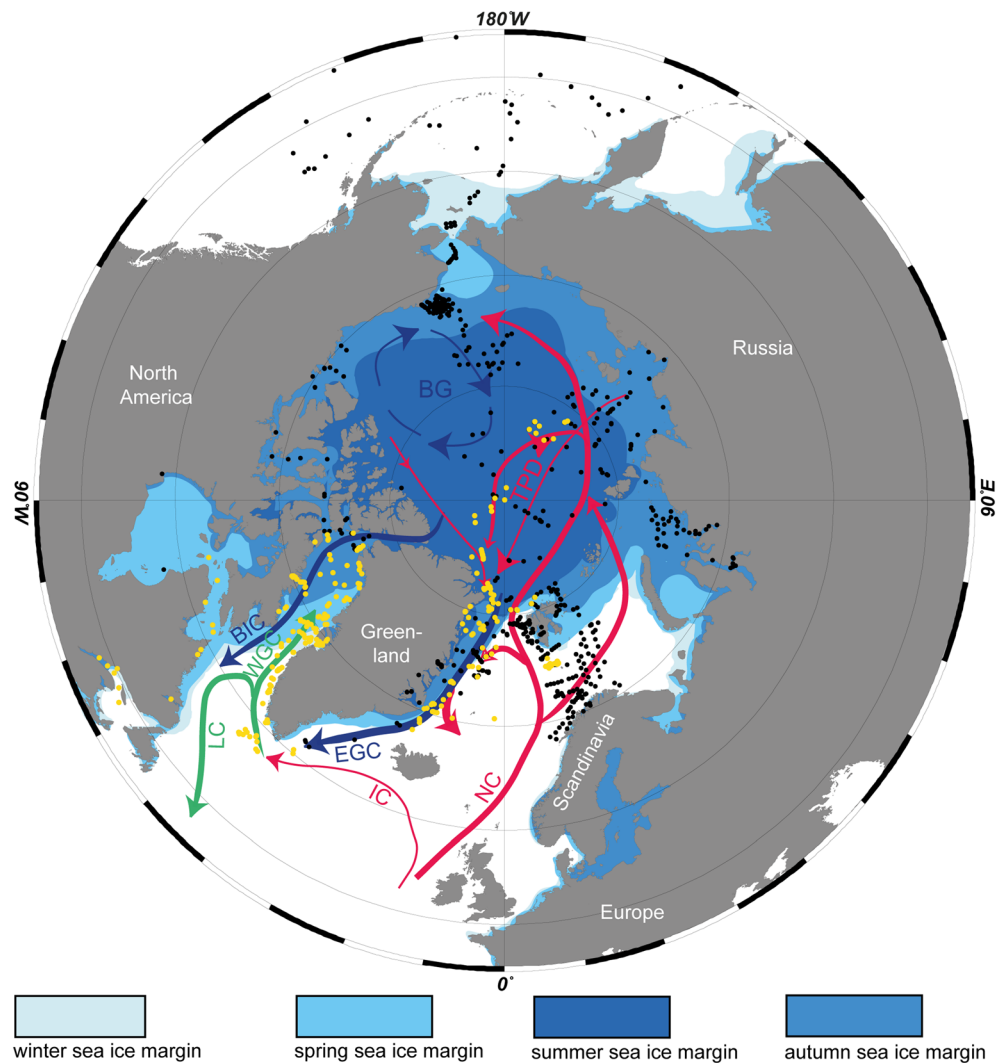
Figure 1. Modern surface circulation in the Arctic Ocean and adjacent regions (adapted after Macdonald et al., 2003). Yellow dots indicate the location of new data from surface sediment samples (this study); black dots indicate the location of previously published data from surface sediment samples (Belt et al., 2007, 2013, 2015; Méheust et al., 2013; Müller et al., 2011; Navarro-Rodriguez et al., 2013; Pieńkowski et al., 2017; Ribeiro et al., 2017; Smik et al., 2016; Wegner Koch et al., 2020; Xiao et al., 2013, 2015). The modern seasonal ice margins are indicated by different shades of blue (Cavalieri et al., 1996, updated 2017). Major surface currents are indicated in red (warm), blue (cold), and green (mixed). Abbreviations are as follows: BIC = Baffin Island Current; BG = Beaufort Gyre; EGC = East Greenland Current; IC = Irminger Current; LC = Labrador Current; NC = Norwegian Current; TPD = transpolar Drift; WGC = West Greenland Current; WSC = West Spitsbergen Current.

the northward flow of warm and saline Atlantic waters carried by the West Spitsbergen Current (WSC) toward the Arctic (Figure 1; Rudels et al., 2005). Sea ice retreats in spring and by summer, only the inner East Greenland Shelf and fjords remain ice-covered while sea ice retreats toward 75–80°N elsewhere in Fram Strait.

The Barents Sea is a shallow shelf area, where sea ice is formed during autumn. It expands from the northeast and reaches its maximum between January and March, extending as far south as 72°N in the eastern basin (Loeng, 1991). Due to the influence of the North Atlantic Current (NAC), the western part of the Barents Sea is less affected by sea ice. Annual variability in NAC intensity accounts for a high variability in annual sea ice extent in the Barents Sea (Kvingedal, 2005).

Another export route of Arctic waters and sea ice is the Canadian Arctic Archipelago and Nares Strait (260.2×10^3 km^2/a; Bi et al., 2019) toward Baffin Bay with the Baffin Island Current (BIC) flowing south along the Canadian Shelf toward the Labrador Sea (Figure 1; Drinkwater, 1996). In the Canadian Arctic Archipelago sea ice is mostly made of landfast ice, which starts to form in October. Sea ice retreats northeastward during spring and summer, while some parts remain ice-covered during the summer months by multi-year ice.

Baffin Bay is mostly ice free in summer and covered by sea ice during autumn and winter (Figure 1; Cavalieri et al., 1996, updated 2017). Here, sea ice starts to form in the northwest to extend southeast (Figure 1). Its maximum is reached in March expanding as far south as 65°N in the western Davis Strait. In eastern Baffin Bay, the inflow of the West Greenland Current (WGC) restricts sea ice extent, as it is composed of the relatively warm Atlantic Irminger Current (IC) mixed with the distal EGC (Figure 1; Cuny et al., 2005; Myers et al., 2007; Tang et al., 2004).

The interplay between the expansion of sea ice, export of polar waters toward the Atlantic, and the inflow of Atlantic-derived waters into the Arctic Ocean characterizes the oceanography and determines the extent of sea ice in sub-Arctic and Arctic shelf seas and basins (e.g., Årthun et al., 2012; Gloersen et al., 1993; Martin & Wadhams, 1999). The presence and formation of sea ice has a major impact on biological primary production in surface waters (Dieckmann & Hellmer, 2008; Wassmann et al., 2011) and seasonal ice margins play an important role in Arctic marine phytoplankton productivity (Sakshaug et al., 2009).

4. Material, Approach, and Methods

4.1. Surface Sediment Samples

The 260 new surface sediment samples presented here were collected during research cruises between 2008 and 2018 (AMD14: Chalut & Merzouk, 2014; HU2008: Campbell & de Vernal, 2009; HU2013: Campbell, 2013; MSM12: Uenzelmann-Neben, 2009; MSM30: Hanebuth, 2009; MSM31: Geissler, 2013; MSM44 and MSM66: Dorschel et al., 2016, 2017; MSM46: Pollehne, 2015; PS87 nad PS93.1: Stein, 2015, 2016; GS15-198: https://www.bcdc.no/files/bcdc-theme/documents/GS15-198_cruise%20report.pdf; GS16-204: https://www.bcdc.no/files/bcdc-theme/documents/GS16204_cruise%20report.pdf; FRAM-2014/2015: Kristoffersen & Tholfsen, 2016; Paaimut2014: Krawczyk et al., 2017; PS109: Kanzow, 2018; PS115.1: Damm, 2019). Grab sampler, giant box corer, and multicorer have been used to retrieve surface sediments in the central Arctic Ocean ($n = 21$), Fram Strait and the East Greenland Margin ($n = 76$), Barents Sea ($n = 24$), Baffin Bay ($n = 115$), and the Gulf of Saint Lawrence ($n = 6$), Hudson Strait ($n = 5$), and Labrador Sea ($n = 13$) between 48°N and 90°N and 79°W and 172°E. All samples were stored in glass vials or plastic bags and were frozen directly after sampling whenever possible. If freezing was not possible directly, samples were stored at 4°C for transportation and were frozen upon arrival. Samples were freeze-dried and stored below −20°C until further treatment.

The new 260 surface sediment samples presented here were analyzed for biomarker content, that is, IP$_{25}$, HBI II, HBI III (Z-isomere and E-isomere), brassicasterol, and dinosterol (see Figures 1–3) and were combined with already published surface sediment biomarker distributions (Belt et al., 2007, 2013, 2015; Navarro-Rodriguez et al., 2013; Méheust et al., 2013; Pieńkowski et al., 2017; Ribeiro et al., 2017, Smik et al., 2016; Wegner Koch et al., 2020; Xiao et al., 2013, 2015) into a (sub-)Arctic comprehensive biomarker surface database (Table 1). For details see supporting information Tables S1 and S2.

4.2. Biomarker Analytics

For geochemical analysis, freeze-dried and homogenized surface sediments were used. Samples were analyzed for total organic carbon (TOC) content and concentrations of the 2,6,10,14-tetramethyl-7-(3-methylpent-4-enyl)pentadecane (IP$_{25}$), 2,10,14-trimethyl-6-enyl-7-(3-methylpent-1-enyl)pentadecene (HBI II), (9Z)-2,6,10,14-Tetramethyl-7-(3-Methylpent-4-enyliden)pendadeca-9-en (HBI III, Z), (9E)-2,6,10,14-Tetramethyl-7-(3-Methylpent-4-enyliden)pendadeca-9-en (HBI III, E), 24-methylcholesta-5, 22E-dien-3β-ol (brassicasterol) and 4 α,23, 24 trimethyl-5α-cholest-22E-en-3β-ol (dinosterol).

Prior to the extraction, two internal standards 7-HND (7-hexylnonadecane, 20 μl/sample), cholesterol-d$_6$ (cholest-5-en-3β-ol-D$_6$; 10.1 μg/sample) and/or androstanol (5α-androstan-3β-ol, 20 μl/sample) were added for quantification purposes. About 5 g of sediment was extracted by sonication (3 × 15 min) with
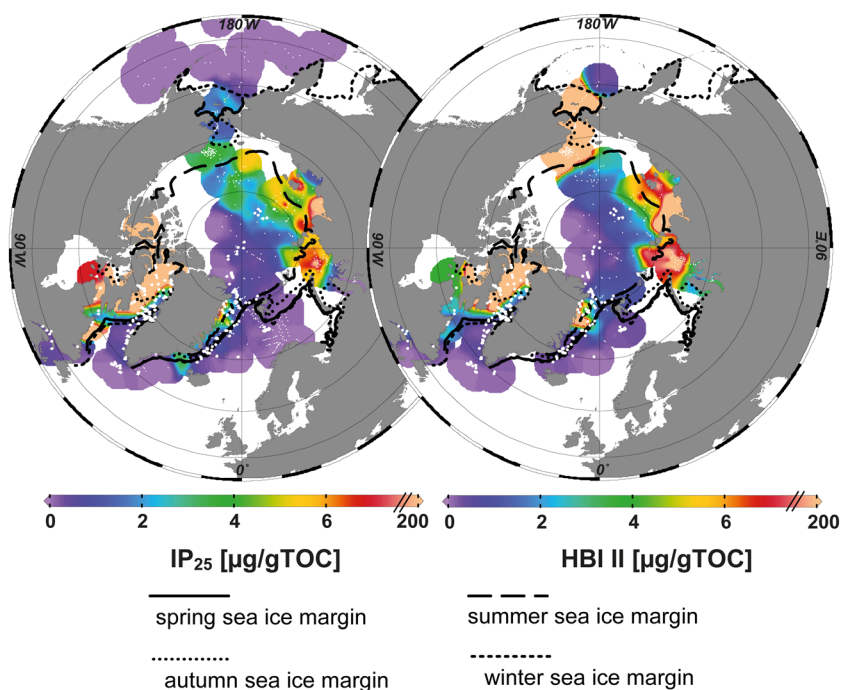
Figure 2. Concentrations of IP$_{25}$ and HBI II (in µg/gTOC) of new (large dots; this study) and published (small dots; Belt et al., 2007, 2013, 2015; Méheust et al., 2013; Müller et al., 2011; Navarro-Rodriguez et al., 2013; Pieńkowski et al., 2017; Ribeiro et al., 2017; Smik et al., 2016; Wegner Koch et al., 2020; Xiao et al., 2013, 2015) surface sediments in the Northern Hemisphere. The seasonal ice margins are indicated by black lines: solid = spring (AMJ); wide dashed = summer (JAS); dotted = autumn (OND); narrow dashed = winter (JFM) (Cavalieri et al., 1996, updated 2017).

dichloromethane:methanol (2:1 vol/vol) as solvent. The extracts were separated in different fractions by open-column chromatography with SiO$_2$ as stationary phase. As solvent n-hexane (5 ml) was used for hydrocarbons and ethylacetate:n-hexane (20:80 vol/vol; 7 ml) for sterols. The sterol fraction was silylated using 200 µl BSTFA (60°C, 2 hr).

Hydrocarbons were analyzed with a gas chromatograph Agilent Technologies 7890 GC (30 m HP-1MS column, 0.25 mm in diameter, and 0.25 µm film thickness) coupled to an Agilent Technologies 5977 A mass selective detector. Sterol concentrations were identified with a gas chromatograph Agilent Technologies 6850 GC (30 m HP-1MS column, 0.25 mm in diameter, and 0.25 µm film thickness) coupled to an Agilent Technologies 5975 A mass selective detector. The studied compounds were identified by comparing their retention times to those of external standards (7-HND, cholesterol-D$_6$/anstrostanol, and reference sediment) by calculating the retention index. IP$_{25}$, HBI II, and HBI III (IP$_{25}$: m/z 350, HBI II: m/z 348, and HBI III (Z/E): m/z 346) were quantified by the abundant fragment ion m/z 266 of the internal standard 7-hexylnonadecane. The sterols were quantified as trimethylsilyl ethers (brassicasterol: m/z 470, dinosterol: m/z 500) in regard to the molecular ion of cholersterol-D$_6$ (m/z 464) or 5α-androstan-3β-ol (ion m/z 348). Instrument stability was controlled by reruns of external standards and replicate analyses for random samples during each analytical sequence.

More detailed measurement settings and compound identification are described by Fahl and Stein et al. (2012). All biomarker concentrations were normalized to both TOC content (µg/gTOC) and gram of sediment (µg/gSed). Biomarker concentrations normalized against TOC have been proven to be more robust in terms of interregional comparison hence we use biomarker concentrations expressed as µg/gTOC. Sedimentary biomarker concentrations in µg/gSed are shown in supporting information Figure S1.

4.3. Combination of Our Data With Previously Published Data Sets

For a detailed Arctic-wide discussion of the biomarker approach, we combined our new data from 260 samples with 615 previously published surface samples from Fram Strait and the East Greenland Shelf (Müller
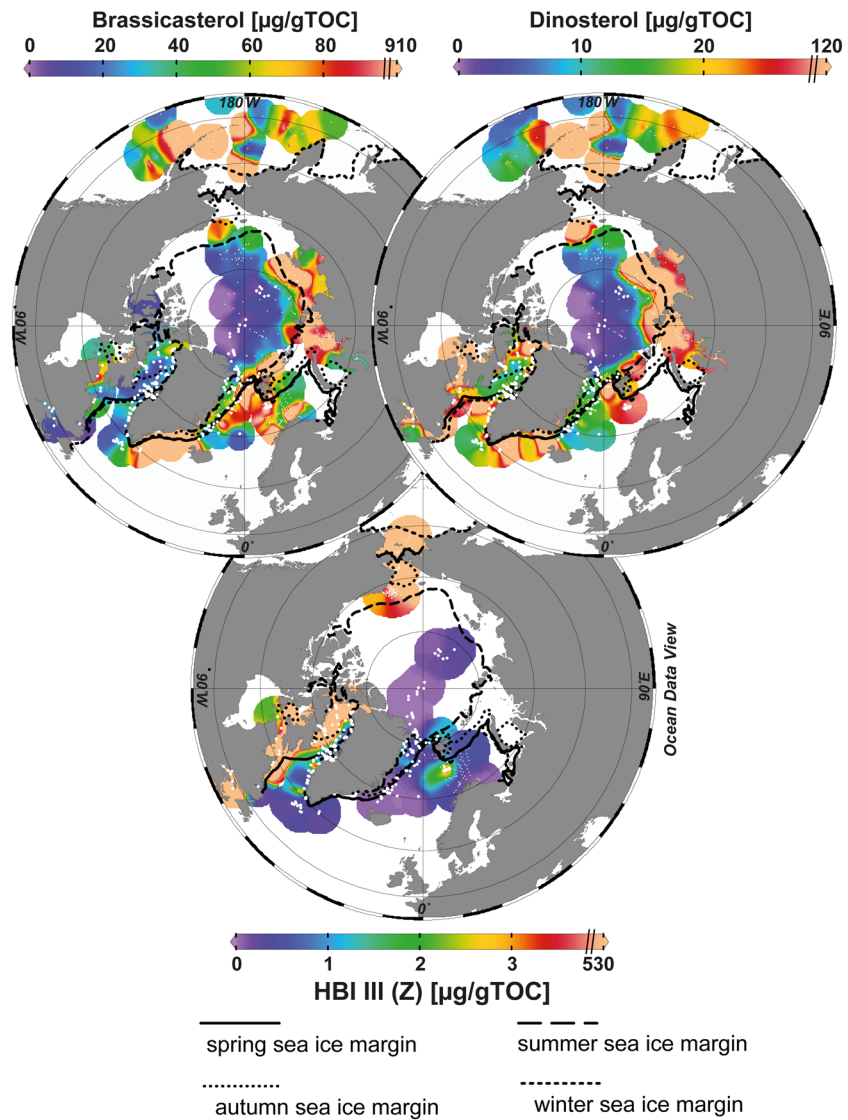
Figure 3. Concentrations of brassicasterol, dinosterol, and HBI III (Z),in µg/gTOC, of new surface sediments (large dots; this study) and published data (small dots; Belt et al., 2007, 2013, 2015; Méheust et al., 2013; Müller et al., 2011; Navarro-Rodriguez et al., 2013; Pieńkowski et al., 2017; Ribeiro et al., 2017; Smik et al., 2016; Wegner Koch et al., 2020; Xiao et al., 2013, 2015). The seasonal ice margins are indicated by black lines: solid = spring (AMJ); wide dashed = summer (JAS); dotted = autumn (OND); narrow dashed = winter (JFM) (Cavalieri et al., 1996, updated 2017).

et al., 2011; Ribeiro et al., 2017; Xiao et al., 2015), Bering Sea (Méheust et al., 2013; Wegner Koch et al., 2020), the Svalbard region and Barents Sea (Belt et al., 2015; Navarro-Rodriguez et al., 2013; Smik et al., 2016; Xiao et al., 2015), the Canadian Arctic Archipelago (Belt et al., 2007, 2013; Pieńkowski et al., 2017), and the central Arctic Ocean and adjacent Russian marginal seas (Wegner Koch et al., 2020; Xiao et al., 2013, 2015) into a (sub-)Arctic database ($n = 875$) (see Table 1 for overview; see supporting information Table S2 for details). With regard to the phytoplankton marker HBI III (Z), we are able to present the first Arctic-wide data set (Figure 3).

A previously published sea ice biomarker data set derived from pan-Arctic surface sediments (Stoynova et al., 2013), which also includes data from Baffin Bay and Hudson Bay, displays biomarker and TOC concentrations that are partly several magnitudes higher than those observed in our Baffin Bay samples and in published surface sediment studies from the Barents Sea and the Arctic Ocean (e.g., Navarro-Rodriguez et al., 2013; Xiao et al., 2015). Stoynova et al. (2013) used different extraction solvents (methylene

chloride:methanol, 9:1) and extraction method (microwave extraction) which was not tested in an interlaboratory study (Belt et al., 2014), the reliability of their results remain unconfirmed. Thus, following Xiao et al. (2015), we excluded the Stoynova et al. (2013) data from our comprehensive data set.

4.4. Environmental Data Set

Modern environmental data used here are sea ice concentration, SST, and salinity, productivity as well as chlorophyll *a* concentration. For sea ice concentration, we used the Nimbus 7 SMMR, SSM/I, and SSMIS passive microwave data set (Cavalieri et al., 1996, updated 2017) provided by the National Snow and Ice Data Centre (NSIDC, n.d.). We also used monthly averages from 1955 to 2017, which include historical observations in addition to satellite measurements from 1979 providing a quasi-complete spatial and temporal coverage (Fetterer et al., 2017). Monthly sea ice concentrations and extent compiled at a (1/4)° resolution are available from NSIDC. For statistical analysis (Chapter 6), SST, sea surface salinity (SSS), chlorophyll *a*, and nutrients are based on the World Ocean Atlas (2013, WOA13). It provides a statistical mean and standard deviation at monthly averaging periods from January 1955 to December 2012 at 1° to (1/4)° spatial resolution for temperature and salinity and at 1° resolution for nitrate, phosphate, and silicate. Bathymetry data are from the International Bathymetric Chart of the Arctic Ocean (Jakobsson et al., 2012) and the *General Bathymetric Chart of the Oceans (GEBCO 2014, version 20141103)* (GEBCO, n.d.).

Primary productivity data are calculated using the vertical generalized production model (VGPM) algorithm applied to the 2002–2019 chlorophyll data provided by *National Aeronautics and Space Administration (NASA)'s Moderate Resolution Imaging Spectroradiometer (MODIS)* program (MODIS, n.d.). The *MODIS* data have a (1/12)° spatial resolution and monthly averages. Data from areas with coverage gaps due to polar night or clouds were filled using simple linear interpolation within an 80 km radius. In Arctic regions, where winter data are missing and Arctic night prevails, we assumed zero primary productivity. Annual and monthly productivity data were downloaded from the *Oregon State University website* (Oregon State University, n.d.).

4.5. Statistical Analysis

Distributional maps of sea ice, biomarker concentrations, sea ice indices, and dinoflagellate cyst data were generated with Ocean Data View (Schiltzer, 2017). Maps were created by using the weighted-average gridding, which uses a variable resolution, depending on the data density (Schlitzer, 2019). Biomarker concentrations are plotted linearly; however, color bars were adjusted to exclude single outliers and highlight biomarker gradients. Outliers with exceptionally high concentrations were excluded and the axis was broken with the highest concentrations shown at the end of the axis.

Multivariate analyses were performed with the Canoco software Version 5 (ter Braak & Šmilauer, 2002) to examine the interrelationship between the different sets of proxy data and the environmental parameters. Detrended correspondence analyses (DCAs) were first used to identify the type of function between dinoflagellate cyst assemblages and environmental variables. Based upon the length of the first axis (number of standard deviations), which is 1.6, the function is rather linear indicating that redundancy analyses (RDAs) is the appropriate technique.

5. Results

Two hundred sixty new sediment surface stations provide biomarker distributions from Baffin Bay, the Labrador Sea, the central Arctic Ocean, Fram Strait, the East Greenland Shelf, and the Barents Sea. In general, the highest IP_{25} concentrations are observed within the seasonal sea ice zone between the maximum and minimum sea ice extent, which we observe in Baffin Bay and the northeast East Greenland Shelf (Figures 2, 4, and 5). By contrast, IP_{25} is absent or only present in lowest concentration in the perennial sea ice-covered central Arctic Ocean as well as in predominantly sea ice-free regions such as the northeastern Labrador Sea, the southeastern Greenland Shelf, and the southern Barents Sea (Figure 2). In Fram Strait, IP_{25} concentrations are low; however, the distribution of IP_{25} in surface sediment samples is mostly related to seasonal sea ice on the East Greenland Shelf (Figure 5).

In our new data, HBI II shows a similar distribution as observed for IP_{25}, as it is absent in the sea ice-free and perennial ice-covered regions (e.g., northeastern Labrador Sea and central Arctic Ocean) and present in seasonally ice-covered regions (e.g., Baffin Bay) (Figure 2).
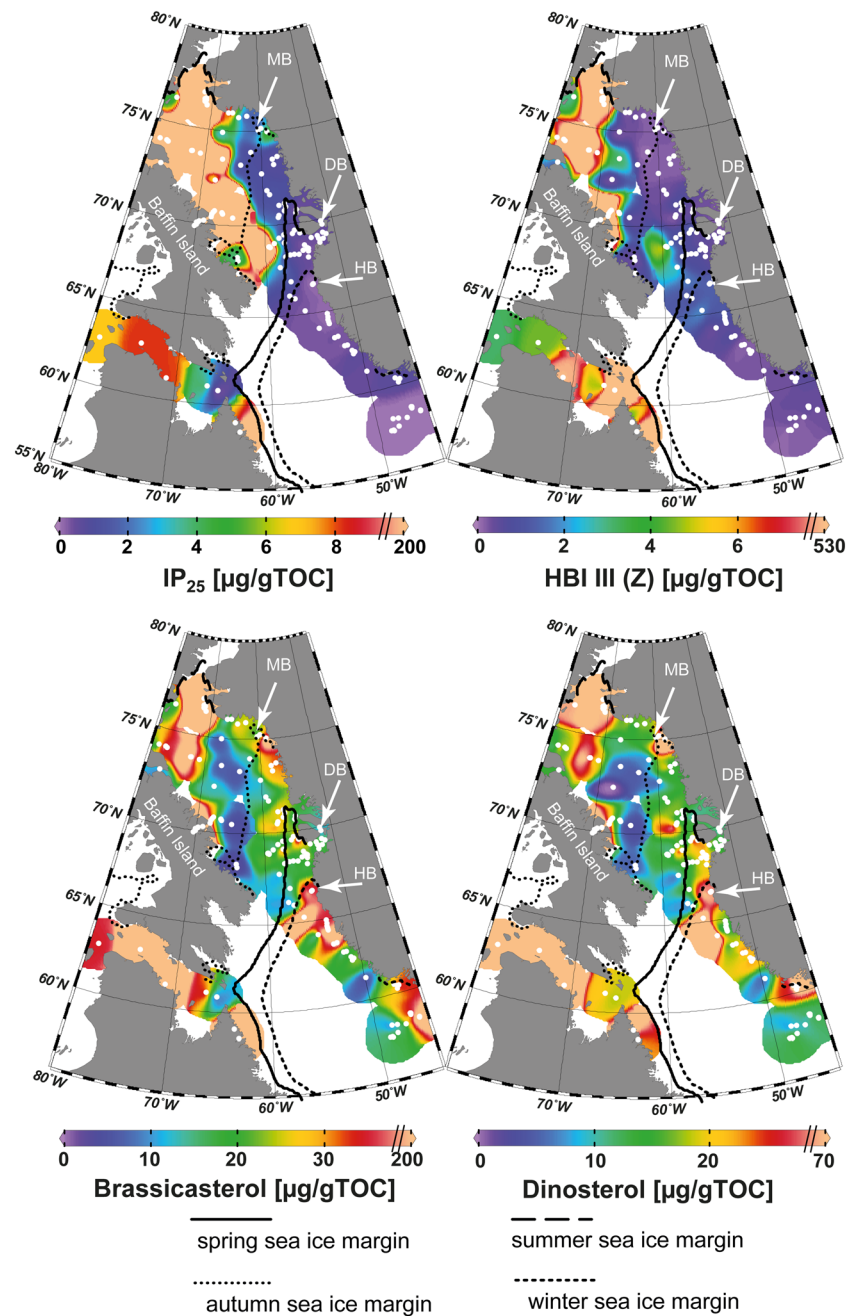
Figure 4. Concentrations of IP$_{25}$, HBI III (Z), brassicasterol, and dinosterol (in µg/gTOC) of new surface sediments (this study) in Baffin Bay. Abbreviations as follows: MB = Melville Bay, DB = Disko Bugt; HB = Hellefiske Banke. The seasonal ice margins are indicated by black lines: solid = spring (AMJ); wide dashed = summer (JAS); dotted = autumn (OND); narrow dashed = winter (JFM) (Cavalieri et al., 1996, updated 2017).

The phytoplankton biomarker HBI III (Z) is absent in the perennially sea ice-covered regions of the central Arctic Ocean but occurs in a few sea ice free areas and in most seasonally ice-covered regions, with highest concentrations in Baffin Bay (Figures 3 and 4). In Fram Strait, the distribution of HBI III (Z) generally corresponds to the spring/winter ice edge (Figure 5). However, in central Fram Strait it is absent in four samples that are situated under or very close to the ice edge (Figure 5). Toward the Russian Shelf, HBI III (Z) is present however in low concentrations (Figure 3). In the Barents Sea, our samples show elevated concentrations, south of Svalbard, close to the spring ice edge (Figure 5).
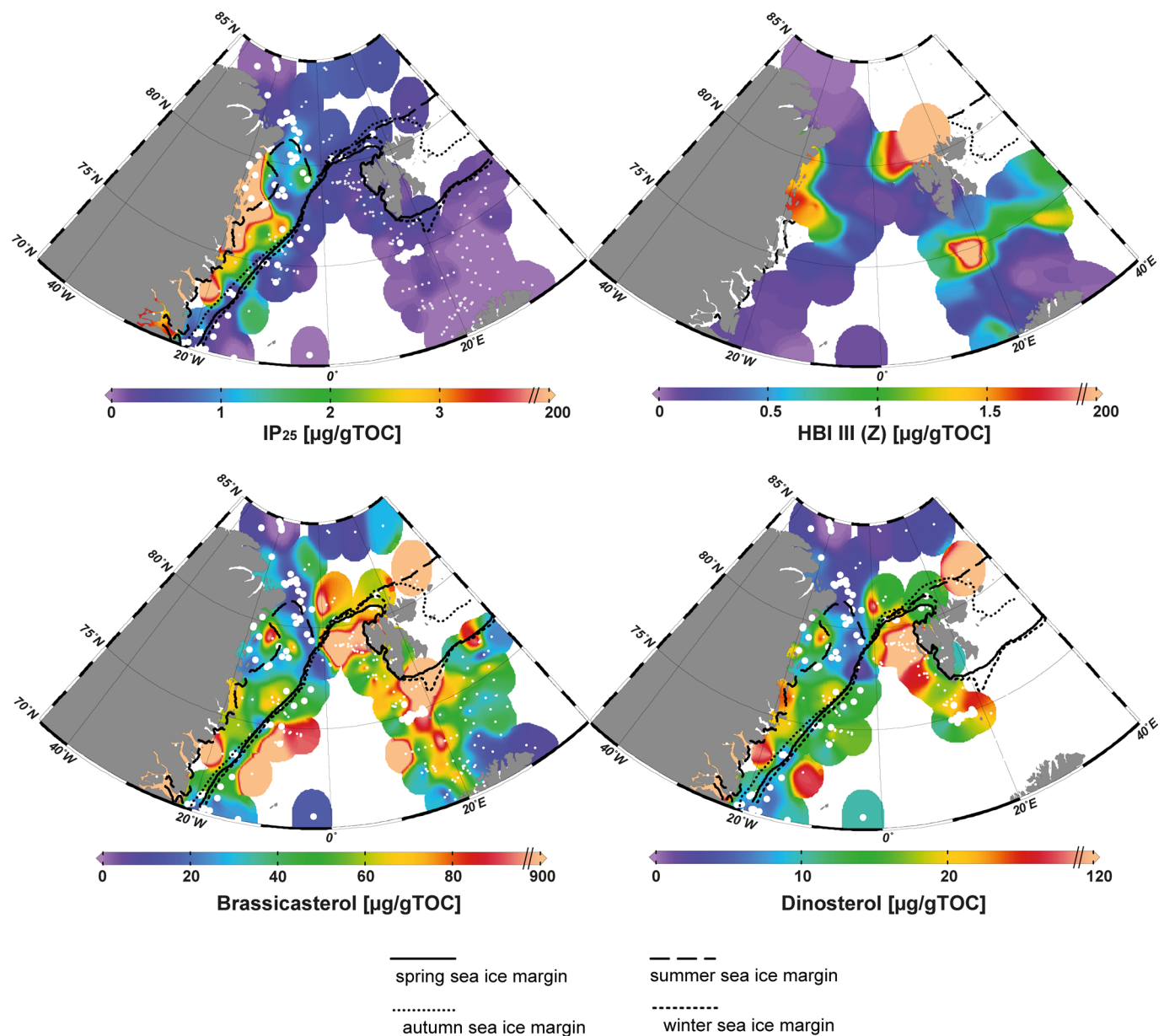
Figure 5. Concentrations of IP$_{25}$, HBI III (Z), brassicasterol, and dinosterol (in µg/gTOC) of new (large dots; this study) and published (small dots; Belt et al., 2015; Müller et al., 2011; Navarro-Rodriguez et al., 2013; Ribeiro et al., 2017; Smik et al., 2016; Xiao et al., 2013, 2015) surface sediments in Fram Strait. The seasonal ice margins are indicated by black lines: solid = spring (AMJ); wide dashed = summer (JAS); dotted = autumn (OND); narrow dashed = winter (JFM) (Cavalieri et al., 1996, updated 2017).

The distribution of the HBI III (E) is similar to that of the Z-isomere and shows a similar distribution pattern (see supporting information Figure S1).

The open-water phytoplankton sterols, brassicasterol, and dinosterol were detected in seasonally sea ice covered and perennially sea ice-free regions (Figure 3). Brassicasterol and dinosterol are mostly absent in sediment samples underlying perennial sea ice cover of the central Arctic Ocean (Figure 3). In Baffin Bay, brassicasterol and dinosterol show high concentrations on the West Greenland Shelf as well as in Nares Strait and off the coast of Baffin Island (Figure 4). In Fram Strait, we find low brassicasterol concentrations toward the central Arctic Ocean and on the northeast Greenland Shelf underlying the cold Arctic water outflow via the EGC (Figure 5). An isolated sample on the northeast Greenland Shelf, in the area of the

Northeast Water (NEW) Polynya, shows elevated brassicasterol concentrations (Figure 5). The distribution pattern of dinosterol is similar to that of brassicasterol, with increased concentrations at the location of the NEW Polynya (Figure 5). Both sterols show similar distributions with the highest concentrations in the Barents Sea and along the flow path of relatively warm and nutrient-rich Atlantic water masses on the west Greenland Shelf (Figures 3 and 5).

6. Discussion

6.1. Pan-Arctic and Regional Biomarker Distributions

Our new surface sediment biomarker record agrees well with previous findings from areas such as the Barents Sea, Fram Strait, the East Greenland Shelf, and the central Arctic Ocean (Belt et al., 2015; Müller et al., 2011; Navarro-Rodriguez et al., 2013; Xiao et al., 2013, 2015). This allows for a combination of our new biomarker distribution record ($n = 260$) with published surface records ($n = 615$; see Table 1 and supporting information Tables S1 and S2) into a pan-Arctic data set ($n = 875$) and a subsequent comparison with modern satellite-derived sea ice conditions. This in turn permits to relate the proxy data to the (regional) extent of perennial and seasonal sea ice (Figures 2 and 3). We are aware that this composite data set may include uncertainties and inconsistencies. First, different sediment treatment (e.g., storage and laboratory method; see Table 1) may affect the quality of the data and may have varying effects on different compounds (Belt, 2018; Belt et al., 2014; Cabedo Sanz et al., 2016). A comparison between the two commonly applied extraction methods (sonication and accelerated solvent extractor [ASE] extraction) revealed that only dinosterol concentration might be affected by the extraction method (supporting information Figure S2). Second, Arctic surface sediment samples may represent a few years up to thousands of years, depending on local sedimentation regimes (see supporting information Figure S3 for overview of local sedimentation rates across the Arctic). Commonly, a first step to address this issue is to normalize biomarker concentrations against TOC to reduce the effect of changing sedimentation rates and other sedimentary processes (cf. Belt & Müller, 2013). The different age representation of surface sediments from different regions or even within some regions cannot be minimized. This in turn may affect the correlation to modern sea ice concentrations (1978–2017; Cavalieri et al., 1996, updated 2017). Hence, we avoid comparing concentrations at single sites but rather focus on general patterns and further discuss the potential influence of sediment ages.

Despite the above-mentioned limitations, the newly compiled biomarker data set illustrates the sensitivity of IP_{25} to the presence of seasonal sea ice. In the central Arctic, IP_{25} is absent, where limited light and nutrient availability restrict ice-algae growth (Gosselin et al., 1997; Walsh, 1989). In the Barents Sea, IP_{25} is mostly absent in the ice-free waters, as observed in previous studies (Belt et al., 2015; Navarro-Rodriguez et al., 2013). High IP_{25} concentrations are found in surface sediments from Baffin Bay, in regions that are seasonally covered by sea ice (Figure 2) with maxima off the coast of Baffin Island, close to the limit of the autumn sea ice extent (Figure 2; Cavalieri et al., 1996, updated 2017), where sea ice remains longest and recurs first. IP_{25} is only present in low concentrations or absent along the southwestern Greenland Shelf, south of the maximum sea ice extent. In western Fram Strait and along the East Greenland Shelf where drift ice from the Arctic Ocean is a predominant feature, IP_{25} is present in low concentrations. The differences between Baffin Bay and Fram Strait, which are both characterized by seasonal sea ice conditions, may be explained by a strong EGC and low nutrient availability on the East Greenland Shelf, hampering productivity (e.g., Hirche et al., 1991). Further, different age representation by sediments from these regions may limit the direct comparison between both regions. In Baffin Bay, it can be assumed that most surface samples from shelf areas represent modern sediments (Krawczyk et al., 2017), whereas sedimentation rates from Fram Strait and the East Greenland Shelf may differ to a large extent depending on the region (e.g., Andrews & Syvitski, 1994; Mienert et al., 1992; Nam et al., 1995; Stein, 2008). Hence, samples from these areas could represent different age intervals, which make a direct comparison difficult.

Another compound that has been discussed in connection with sea ice is HBI II (Belt et al., 2007; Massé et al., 2011; Vare et al., 2009). It has been reported to occur in some ice-free regions, such as the Everglades in Florida, for example (Barrick & Hedges, 1981; He et al., 2016; Summons et al., 1993; Volkman et al., 1983; Yruela et al., 1990). However, in our data set, which is mostly comprised of sediment samples in sea ice-affected regions, HBI II is absent in ice-free regions, for example, south of Greenland. This supports conclusions from other studies (Fahl & Stein, 2012; Massé et al., 2011; Vare et al., 2009; Xiao

et al., 2013, 2015). There are, however, distinct regional differences. For example, we find a positive correlation between HBI II and IP_{25} in Fram Strait (supporting information Figure S4.2), which is not the case in Baffin Bay (supporting information Figure S4.3). This points to some regionally different, yet unknown conditions under which HBI II and IP_{25} are produced. Nevertheless, it does not rule out an adaption of findings from the Southern Hemisphere (Belt et al., 2017), where HBI II is produced by sea ice dwelling diatoms that live in seasonal sea ice in shelf areas. In the Northern Hemisphere, however, further work is needed in this regard.

In context with the reconstruction of Arctic sea ice and open-water conditions, brassicasterol is often used as open-water phytoplankton biomarker (e.g., Müller et al., 2009, 2011; Xiao et al., 2015). Belt et al. (2015) suggested that brassicasterol might also be produced by sea ice algae to a certain extent. In our study, however, we find no obvious relationship with IP_{25} (supporting information Figure S4.1). Hence, we assume that if brassicasterol is produced by sea ice algae, this makes up only an insignificant proportion of the overall brassicasterol production, which does not notably affect the results of the $P_B IP_{25}$ index calculation. A terrestrial source for brassicasterol, as described in some studies from the Laptev and Kara Seas off major river mouths, seems to be more relevant on a local scale (e.g., Fahl et al., 2003; Hörner et al., 2016). Thus, brassicasterol may be used as an open-water phytoplankton biomarker, but potential local and regional alternative sources need to be considered.

The distribution of HBI III (Z) in the (sub-)Arctic data set, supports findings from Antarctica where HBI III (Z) concentrations in surface sediments from the MIZ are several magnitudes higher than in ice-free regions (Belt et al., 2015). It is also consistent with studies from the Barents Sea where high concentrations of HBI III (Z) in the same region have been associated with the retreating ice edge (Belt et al., 2015; Smik et al., 2016). In the newly compiled (sub-)Arctic data set we find HBI III (Z) and IP_{25} mostly within a similar concentration range, as reported earlier from the Barents Sea, which makes the use of HBI III (Z) advantageous for calculating the PIP_{25} index as compared to brassicasterol and dinosterol (Belt et al., 2015; Smik et al., 2016). However, in some regions, such as the northeast Greenland Shelf, we find extensive differences between concentrations of these biomarkers (Figures 2 and 3), which would require a balance factor to calculate the $P_{III} IP_{25}$ index. The coverage of the HBI III (Z) data set is still incomplete with some data gaps in Arctic shelf areas, which prevent firm conclusions to be made in this regard.

Based on multivariate analysis (Figure 7a), we do not find a significant effect of water depth on IP_{25} or any of the PIP_{25} indices. This indicates that even if IP_{25} concentrations may decrease with water depth due to degradation and remineralization processes (Belt & Müller, 2013; Fahl & Stein, 2012), bathymetry does not influence the trend in this specific biomarker signal significantly. For brassicasterol and dinosterol we find a negative correlation to water depth (Figure 7a), which may point toward high productivity in shelf areas compared to the open ocean (Whitney et al., 2005). However, other effects, such as pelagic grazing and nutrient recycling within the photic zone, may also affect the sedimentary signal of biomarkers. At this point, this seems unlikely, as it should affect all biomarkers similarly.

RDA shows correlations of IP_{25} with spring sea ice. Further correlations of brassicasterol and dinosterol with different nutrients were found (Figure 7). The strength of correlation with silica and nitrate depends upon the data set used. On one hand, we observe a correlation between brassicasterol, dinosterol, and silica in the larger data set ($n = 427$; all samples with TOC, IP_{25}, brassicasterol, dinosterol, and PIP_{25} indices). On the other hand, the smaller data set ($n = 176$; all samples with data for all investigated biomarkers/indices) shows a correlation between both sterols and nitrate. We assume that this may be caused by a regional effect. The smaller data set mostly includes samples from our new record of the Baffin Bay and the East Greenland Shelf, whereas the larger data set includes a large surface data set including the Barents Sea and Russian shelves (Xiao et al., 2013, 2015). The Russian shelves are characterized by river outflow, carrying high concentrations of nitrate whereas the (sub-)Arctic North Atlantic is dominated by northward flowing low-nutrient surface water (Sakshaug et al., 2009). Furthermore, the Barents Sea is largely depleted in silicate (Popova et al., 2010). We assume that for the smaller data set, nitrate is a major limiting factor, whereas the larger data set includes areas with high riverine nitrate input and silica depletion. Hence, nitrate is less limiting in the large data set, and silica limitation may become more pronounced.

Depending upon the data set we used, a negative or positive correlation is observed between brassicasterol and dinosterol and salinity (Figure 7). Again, we assume this may be caused by regional signals. The larger data set includes a large number of samples from the Russian shelves and central Arctic Ocean, where extremely low salinities (WOA, 2013) due to fluvial input und sea ice melt that may affect phytoplankton productivity, thus brassicasterol and dinosterol concentrations. In the smaller data set that mainly includes samples from the East Greenland Shelf and Baffin Bay, salinities are nor as variable (WOA, 2013) and are ordinated together with temperature and productivity, while they are in opposition with sea ice. Hence, there seems to be an opposition between oceanic productivity signal (high salinity and temperature) and sea ice environments marked by reduced phytoplankton bloom and high rates of glacier/sea ice melt.

6.1.1. Biomarker Indices for Environmental Reconstructions

The ratio of the HBI II to IP_{25} (DIP_{25} index; Cabedo-Sanz et al., 2013; supporting information Figure S5) has been discussed as a possible index for SST (Cabedo-Sanz et al., 2013; Fahl & Stein, 2012; Müller & Stein, 2014; Stein et al., 2012; Xiao et al., 2013). However, based on RDA, we find no significant relationship between the DIP_{25} index and SSTs (Figure 7b). While both HBI II and IP_{25} are associated with seasonal sea ice, our data do not support a significant temperature sensitivity of the DIP_{25} index. This is in line with Belt et al. (2018) who postulate that a relationship to SST seems to be unlikely given the near-uniform temperatures found at the base of seasonal sea ice where IP_{25} and HBI II are biosynthesized.

For the newly developed TR_{25} ratio we do not find a clear correlation to spring phytoplankton chlorophyll a concentrations in Baffin Bay and Fram Strait, as was found in the Barents Sea surface sediments by Belt et al. (2019) (supporting information Figure S6). In Baffin Bay, however, we find high TR_{25} values parallel to the spring/autumn/winter ice edges. RDA results of all available TR_{25} data support our findings and seem to indicate a link to spring productivity (Figure 7b). Our results support in part findings by Belt et al. (2019) from the Barents Sea. Nevertheless, our results show that the application of the TR_{25} index is more challenging when applied in different regions. To further develop this index, extensive work is needed to investigate the relationship between Z-isomere and E-isomere of HBI III with chlorophyll a concentrations in different regions.

The PIP_{25} index has been shown to be a useful tool for semiquantitative sea ice reconstructions (Müller et al., 2011; see Belt, 2018, for review). However, the balance factor is one of the main uncertainties of this approach as discussed previously (Belt et al., 2015; Smik et al., 2016; Xiao et al., 2015). To further test the influence of the balance factor on the reliability of the PIP_{25} index in terms of sea ice reconstruction, we compare the correlations of PIP_{25} indices calculated with a regional c-factor and a (sub-)Arctic c factor with seasonal sea ice concentrations (see supporting information Table S2 for details), using the comprehensive biomarker database. This approach is especially relevant for the $P_{III}IP_{25}$ index, which uses HBI III (Z) as phytoplankton marker, which made the balance factor irrelevant due to similar concentrations of HBI III (Z) and IP_{25} in the Barents Sea area (Belt et al., 2015; Smik et al., 2016). In general, our results indicate a (sub-)Arctic c factor as the more reliable approach when using brassicasterol and dinosterol as phytoplankton markers, supported by previous findings by Xiao et al. (2015). When using HBI III (Z) as phytoplankton marker, we find highest correlations to modern sea ice concentrations when using $c = 1$ (see supporting information Table S2). This supports local studies from the Barents Sea (Belt et al., 2015; Smik et al., 2016). However, our data illustrate that HBI III (Z) and IP_{25} show concentration differences in certain areas, such as the central Arctic Ocean and some parts of the northeastern Greenland Shelf. This becomes especially evident when calculating the balance factor for the complete data set ($c = 0.65$) and for the East Greenland Shelf and Fram Strait ($c = 3.31$) (supporting information Table S2A). Based on these findings, we advise caution when using the $P_{III}IP_{25}$ index, especially in a paleocontext, until further studies from various regions provide additional information on HBI III (Z) and IP_{25} concentration differences/similarities under different environmental settings.

All PIP_{25} indices are broadly consistent with the sea ice extent from 1978–2017 (Cavalieri et al., 1996, updated 2017; Figure 6) and show highest correlations to autumn sea ice. Further, $P_{B}IP_{25}$ and $P_{D}IP_{25}$ show high correlations to spring and winter sea ice (Table 2). Canonical RDAs provide significant correlations of all PIP_{25} indices with spring sea ice concentration (Figure 7). Yet the individual correlations of each index differ between regions, which indicate that they may reflect sea ice concentrations from different seasons (see further discussion below). In this regard, it should be noted that the treatment of satellite sea ice data
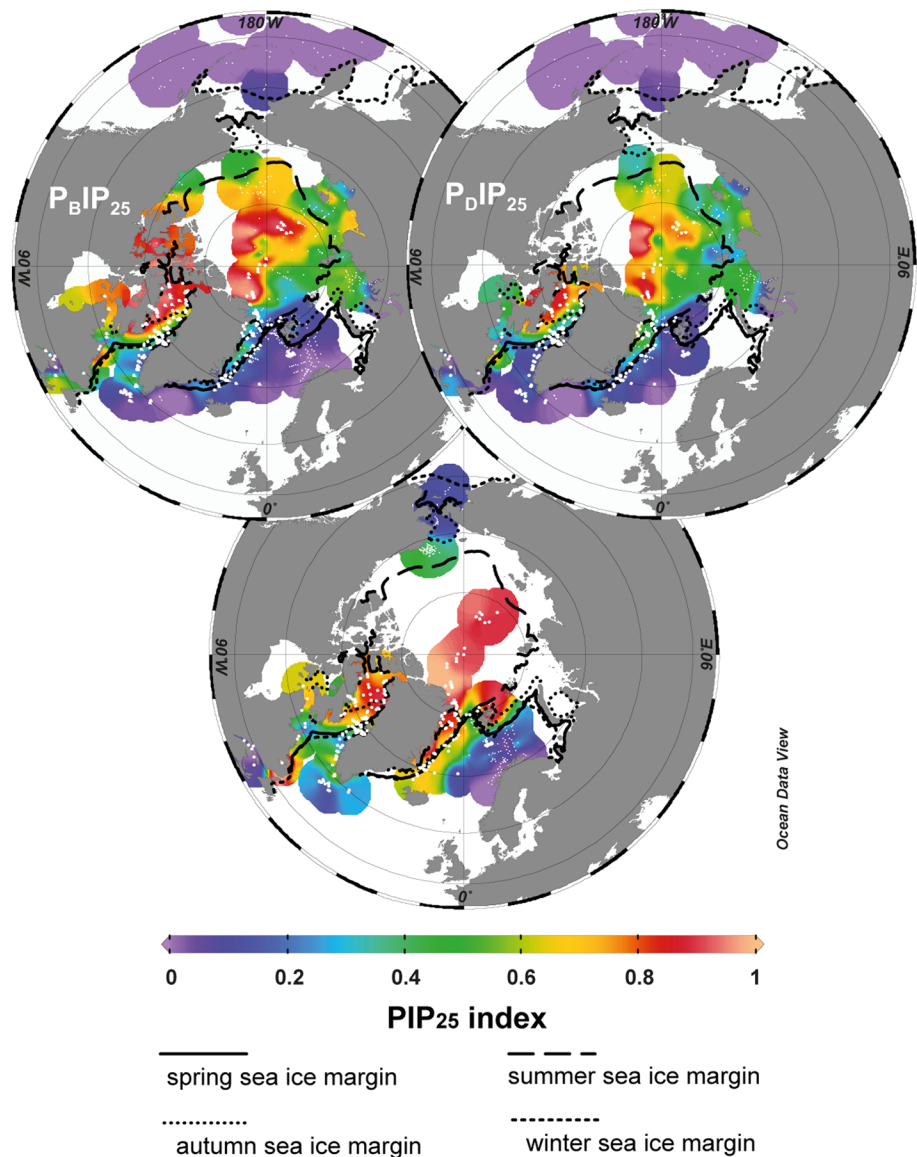
Figure 6. New (large dots; this study) and published (small dots; Belt et al., 2007, 2013, 2015; Méheust et al., 2013; Müller et al., 2011; Navarro-Rodriguez et al., 2013; Pieńkowski et al., 2017; Ribeiro et al., 2017; Smik et al., 2016; Wegner Koch et al., 2020; Xiao et al., 2013, 2015) values of the PIP_{25} indices using brassicasterol (P_BIP_{25}), dinosterol (P_DIP_{25}), and HBI III (Z) ($P_{III}IP_{25}$). The seasonal ice margins are indicated by black lines: solid = spring (AMJ); wide dashed = summer (JAS); dotted = autumn (OND); narrow dashed = winter (JFM) (Cavalieri et al., 1996, updated 2017).

has a significant influence on these results. Belt et al. (2019) used the same data set but took a different sea ice concentration as reference for sea ice margins (this study 50%; Belt et al., 2019: 0%), which influences the visual comparison but does not affect the correlations between PIP_{25} indices and satellite-derived sea ice concentrations. Further, the time interval of observed sea ice concentrations used for the comparison with proxy data is of great importance. Often, the time interval between 1980 and 2000 is used to compare satellite observations with proxy records, as this time interval largely excludes the modern sea ice decline (Swart et al., 2005). We observe no clear improvement in the correlations between PIP_{25} indices and sea ice concentrations when using this time interval (supporting information Table S3C). Hence, for the following discussion we will use the 1978–2017 NSIDC data set. Correlations of PIP_{25}-based sea ice reconstructions with the 1980–2000 sea ice data set do not indicate a clear relationship with autumn sea ice concentrations, whereas the correlation with the 1978–2017 sea ice data set suggest a particularly

Table 2
Correlation Coefficient (r) Between PIP$_{25}$ Indices With Sea Ice Concentrations From the Extended Comprehensive Data Set

Season	P$_B$IP$_{25}$	P$_D$IP$_{25}$	P$_{III}$IP$_{25}$
Spring	0.65	0.64	0.47
Summer	0.57	0.56	0.52
Autumn	0.70	0.67	0.63
Winter	0.63	0.60	0.50

strong relationship autumn sea ice concentrations (see Table S3). This may point toward a prolongation of the bloom seasons or a new autumn bloom in the (sub-)Arctic realm due to sea ice loss (e.g., Ardyna et al., 2014).

The suitability of different phytoplankton markers as indicators for ice-free conditions is a matter that has been discussed previously, especially in regard to the calculation of the sea ice index PIP$_{25}$ (Belt et al., 2015; Navarro-Rodriguez et al., 2013; Smik et al., 2016; Xiao et al., 2013, 2015). Based on our newly compiled pan-Arctic data set, we find consistent correlations of all PIP$_{25}$ indices on a (sub-)Arctic scale. The P$_{III}$IP$_{25}$ ($n = 593$) and P$_D$IP$_{25}$ ($n = 489$) databases have a lower sample density that may limit the direct comparison. Further, the application of the PIP$_{25}$ indices for paleoreconstructions needs caution. We recommend calculating a balance factor for each core, as phytoplankton and sea ice marker ratios may differ from modern values throughout geological time scale. Additionally, the represented sea ice season may not always be spring, as we show that high correlations are
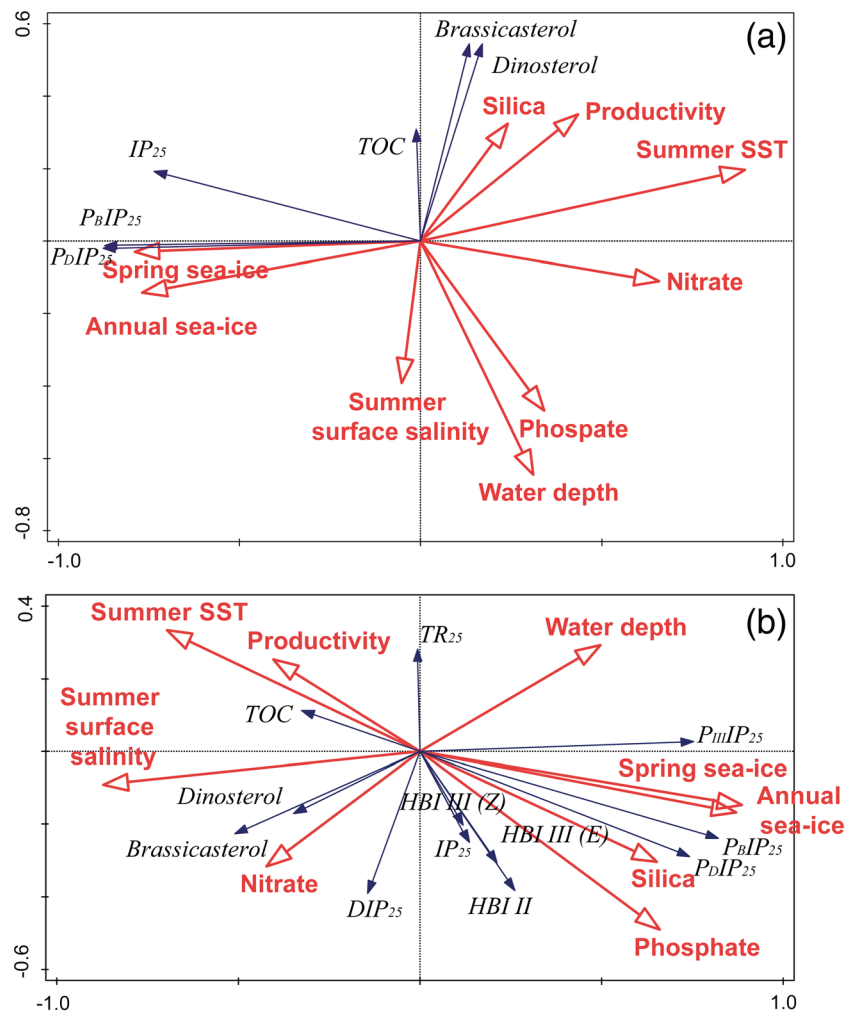

Figure 7. Results from multivariate analysis illustrating the interrelationships between concentrations of biomarkers (in µg/g sediment) and indices, that is, P$_B$IP$_{25}$, P$_D$IP$_{25}$, P$_{III}$IP$_{25}$, and TOC (in %) and selected environmental variables. The environmental parameters include summer sea surface temperature (SST), productivity (gC/m^2/yr), water depth (m), summer salinity, annual sea ice concentration (month/yr), spring sea ice concentration (%), and specific nutrients. For (a) 427 samples and (b) 176 samples that include HBI II and HBI III (Z-isomere and E-isomere) and the indices DIP$_{25}$, P$_{III}$IP$_{25}$, and TR$_{25}$.

also found with autumn and winter sea ice concentrations. Regional settings and individual biomarker concentrations need to be considered. Here, the $P_{III}IP_{25}$ and P_DIP_{25} databases should be extended as they indicate good correlations, but a wider spatial distribution is needed to verify their potential. Especially, in regard to the $P_{III}IP_{25}$ index, further work is needed to investigate the redundancy of the balance factor in its calculation on a wider spatial distribution.

This subject is discussed in the following sections for two regions characterized by high seasonal sea ice variability, Baffin Bay and Fram Strait, where the comprehensive (sub-)Arctic data set displays a good spatial sample coverage for all PIP_{25} indices.

6.2. Baffin Bay

The distribution of IP_{25} and the investigated phytoplankton biomarkers are closely related to the strongly variable sea ice conditions in Baffin Bay. HBI III (Z) in surface sediments from Baffin Bay shows highest concentrations in the northwest, off Baffin Island, where sea ice remains longest throughout the year (Figure 4), which are located both close to the spring ice edge (Myers et al., 2007; Tang et al., 2004) and on the Canadian Shelf, where strong winds promote deep mixing and nutrient upwelling during autumn (Humlum, 1985). Lowest concentrations are observed in the deeper central Baffin Bay where sea ice remains longest during summer (Figure 4). This may be caused by the extensive sea ice cover, which hampers productivity and causes lower sedimentation rates than observed on the high-productivity West Greenland Shelf (e.g., Krawczyk et al., 2017, Simon et al., 2016), which may cause these sediments to be older than those on the shelf. Its distribution supports the association of HBI III (Z) to productivity along the MIZ as suggested by Belt et al. (2015) from the Barents Sea. However, HBI III (Z), which is assumed to be produced by the marine diatom genus *Rhizosolenia* (Belt et al., 2017), is not found in all surface sediment samples from our study area. It is absent in Melville Bay (Figure 4), which may be explained by phytoplankton bloom seasonality and sea ice conditions in this specific area. Sea ice edge conditions in Melville Bay prevail mostly in June while sea ice retreats northward. When sea ice forms again in October/November, it expands fast without the formation of a stable ice edge in Melville Bay (Cavalieri et al., 1996, updated 2017). Furthermore, the phytoplankton community in Baffin Bay records large changes throughout the year. While diatoms dominate the phytoplankton community, their population is strongly reduced during spring and early summer (e.g., Jensen & Christensen, 2014). Our assumption that HBI III (Z) is not produced in this specific area due to a combination of a very short ice edge season that overlaps with a shift in phytoplankton community is supported by a study of northeastern Greenland fjord surface sediments. Ribeiro et al. (2017) showed a clear positive correlation between diatom abundances and HBI III (Z) concentrations. In this context it has to be kept in mind that the producers of HBI III (Z) are still not completely known, and further work is needed in this regard.

The phytoplankton sterols brassicasterol and dinosterol show similar distributions as HBI III (Z) in surface sediments from Baffin Bay (Figure 4). Highest concentrations are found on the West Greenland Shelf, along the flow path of relatively warm and nutrient-rich Atlantic water masses (Myers et al., 2007; Tang et al., 2004) and on the Canadian Shelf. It appears that a combination of seasonal stratification, nutrient availability and sea ice distribution control brassicasterol and dinosterol production, as they are produced by a wide range of open-water phytoplankton organisms (Volkman, 1986; Volkman et al., 1993). Based on their respective distribution, we suggest that HBI III (Z) is mainly produced in the MIZ whereas brassicasterol and dinosterol are mostly driven by open-water conditions and nutrient availability.

In Baffin Bay, the P_BIP_{25} and P_DIP_{25} indices correlate with spring and autumn sea ice concentrations ($r > 0.8$) but show also high correlations to those of winter (Figure 8 and Table 3). This may be related to the broad source of brassicasterol and the fact that Baffin Bay experiences two main phytoplankton blooms, in spring and autumn (Krawczyk et al., 2015). The $P_{III}IP_{25}$ index correlates strongest with spring sea ice and also shows correlations to autumn and winter sea ice concentrations (Table 3), whereas its correlation is of lesser significance compared to the other two indices. This may be related to the absence of HBI III (Z) in Melville Bay, which results in an overestimation of the sea ice conditions by the $P_{III}IP_{25}$ index (Figure 8). It should be noted that all indices show low correlations with summer sea ice concentrations (Table 3). The correlation to winter sea ice may be caused by similar sea ice extent as observed during spring as phytoplankton production is restricted by light during winter.
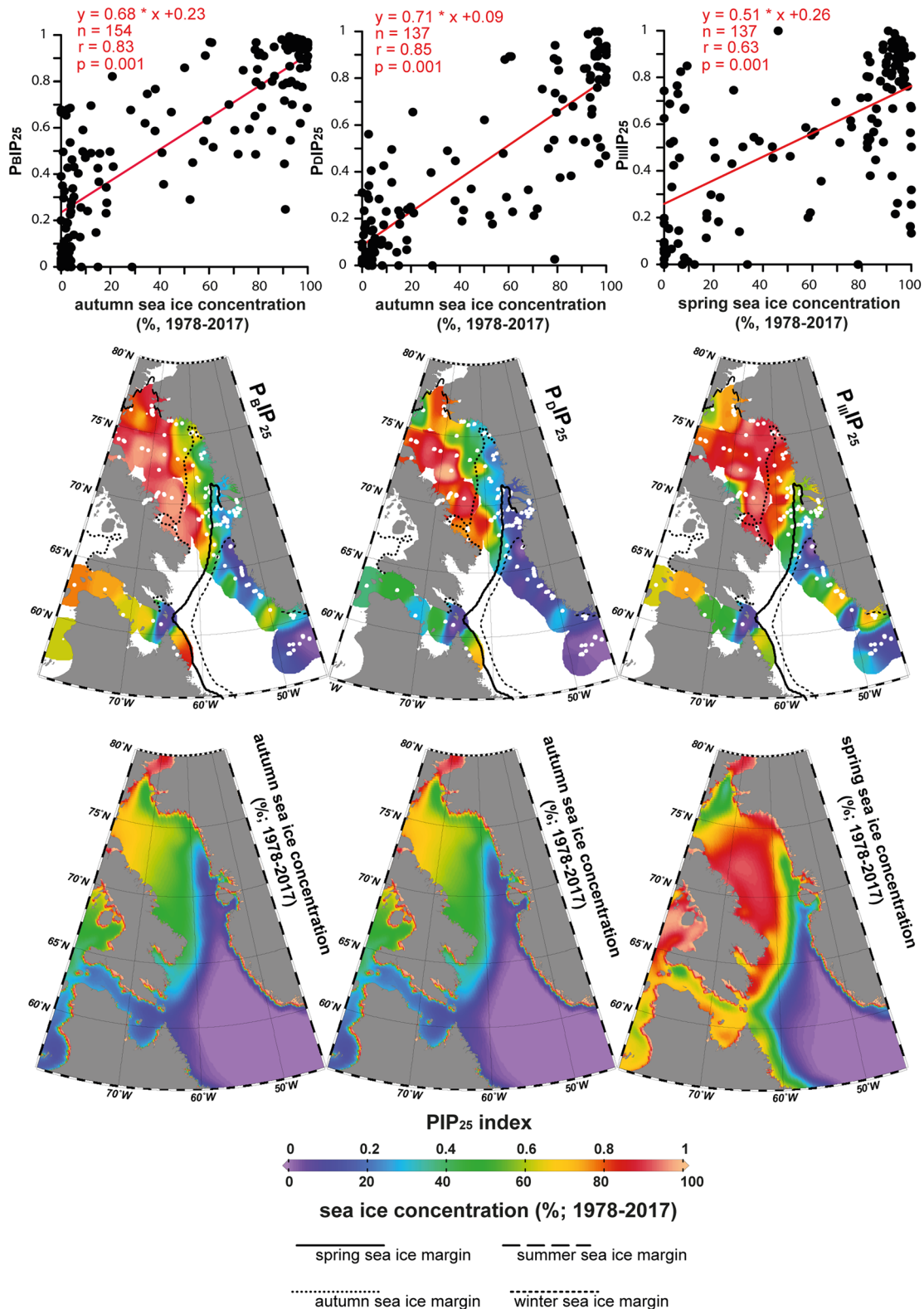
Figure 8. Comparison of sea ice reconstructions using P_BIP_{25}, P_DIP_{25}, and $P_{III}IP_{25}$ with the seasonal sea ice distribution in Baffin Bay. The upper panels show correlations of the specific sea ice reconstruction to spring sea ice concentrations (Cavalieri et al., 1996, updated 2017). The middle panels show the spatial distribution of PIP_{25} indices in Baffin Bay; white points indicate location of surface samples (this study). Abbreviations as follows: MB = Melville Bay, DB = Disko Bugt; HB = Hellefiske Banke. Panels below show the corresponding sea ice concentrations of those seasons with the highest correlations with PIP_{25} values (Cavalieri et al., 1996, updated 2017).

Table 3

Correlation Coefficient (r) Between PIP_{25} Indices With Sea Ice Concentrations From Baffin Bay for Different Seasons

Season	P_BIP_{25}	P_DIP_{25}	$P_{III}IP_{25}$
Spring	0.80	0.76	0.63
Summer	0.55	0.55	0.28
Autumn	0.83	0.85	0.57
Winter	0.79	0.77	0.58

6.3. Fram Strait and East Greenland Margin

IP_{25} distribution in Fram Strait is characterized by the inflow of warm Atlantic Water from the south hampering the production of sea ice (Rudels et al., 2005; Figures 1 and 5). East of Svalbard, IP_{25} is nearly absent even though this area is covered by sea ice in winter and spring. Fast sea ice retreat in summer, unfavorable light conditions in autumn and harsh sea ice conditions throughout most of the year (Cavalieri et al., 1996, updated 2017) possibly result in unfavorable conditions for blooms of diatom species producing IP_{25}, which seem to be generally associated with the winter/spring ice edge. Besides seasonal sea ice and local IP_{25} production, allochthonous input from melting Arctic drift ice exported from the Arctic Ocean may contribute to the IP_{25} signal along the East Greenland Shelf (Aagaard & Coachman, 1968a, 1968b).

HBI III (Z) distribution in Fram Strait seems closely related to the low-nutrient regime of the EGC (e.g., Aagaard & Coachman, 1968a, 1968b; Hopkins, 1991; Johannessen et al., 1999) or yet unknown processes. A higher sample resolution preferably with age control, the same sample treatment concerning sampling, storage, and extraction method along the East Greenland Shelf, is necessary to adequately evaluate the production of HBI III (Z) in Fram Strait and the Greenland Sea.

High brassicasterol and dinosterol concentrations reflect increased open-water phytoplankton productivity in areas of warm nutrient-rich Atlantic Water pathways in the Barents Sea, eastern Fram Strait and south off the ice edge in the Greenland Sea. In general, the cold, nutrient-depleted water masses and harsh sea ice conditions along the northeast Greenland Shelf hamper open-water phytoplankton production (Aagaard & Coachman, 1968a, 1968b; Hopkins, 1991; Johannessen et al., 1999; Müller et al., 2011).

The sea ice cover in Fram Strait shows a much smaller spatial variation throughout the year than Baffin Bay, with a rather narrow zone of seasonal sea ice cover between perennial sea ice and year-round open waters. Furthermore, Fram Strait is located farther north, which reduces the light availability throughout the year and limits phytoplankton productivity to a short season from spring to early autumn. Hence, the PIP_{25} indices in this area show different correlations to modern sea ice conditions than those of Baffin Bay (Table 4). We calculate a relatively high correlation coefficient between all PIP_{25} indices with autumn sea ice concentrations (Table 4). However, the correlations to the other seasons are also high. The differences between seasonal correlations to sea ice are not as pronounced as in Baffin Bay, which may relate to the smaller spatial variability of seasonal sea ice in Fram Strait. Further, a shorter bloom season, compared to, for example, Baffin Bay, may cause this effect. Another effect that may influence the correlations between the PIP_{25} signal and modern sea ice concentrations in this area is the high variability in sedimentation rates and a possible difference in age representation between samples. High sedimentation rates are usually observed in fjords and the central Fram Strait (e.g., Andrews & Syvitski, 1994; Perner et al., 2015; Stein, 2008) and low rates toward the East Greenland Shelf edge and toward the outer Fram Strait (Mienert et al., 1992; Stein, 2008). We expect sediments in this area to represent diverse age ranges, which makes a correlation to a specific interval more difficult than in other regions.

The P_BIP_{25} and P_DIP_{25} indices show relatively low values in the area of the NEW Polynya, which opens during summer and autumn (Schneider & Budéus, 1997), supporting our hypothesis of both indices reflecting at least in parts autumn sea ice conditions. Even though the $P_{III}IP_{25}$ index shows also the highest correlation to autumn sea ice it does not reflect the NEW Polynya (Figure 9). This could be related to the low concentrations of HBI III (Z) in the NEW Polynya region, causing $P_{III}IP_{25}$ to overestimate sea ice conditions in this area (Figures 5 and 9). As observed in Baffin Bay, relatively high correlations of all PIP_{25} indices are observed for winter sea ice concentrations, which could be explained by a similar sea ice extent in spring and the phytoplankton production restriction due to light conditions during winter.

6.4. Toward Biogenic Proxies of Seasonal Sea Ice Concentrations

In addition to biomarker reconstructions, dinoflagellate cysts have been used in another sea ice proxy approach for Northern Hemisphere-wide

Table 4

Correlation Coefficient (r) Between P_BIP_{25}, P_DIP_{25}, and $P_{III}IP_{25}$ Indices From Fram Strait, Barents Sea, and the Greenland Margin for Different Seasons

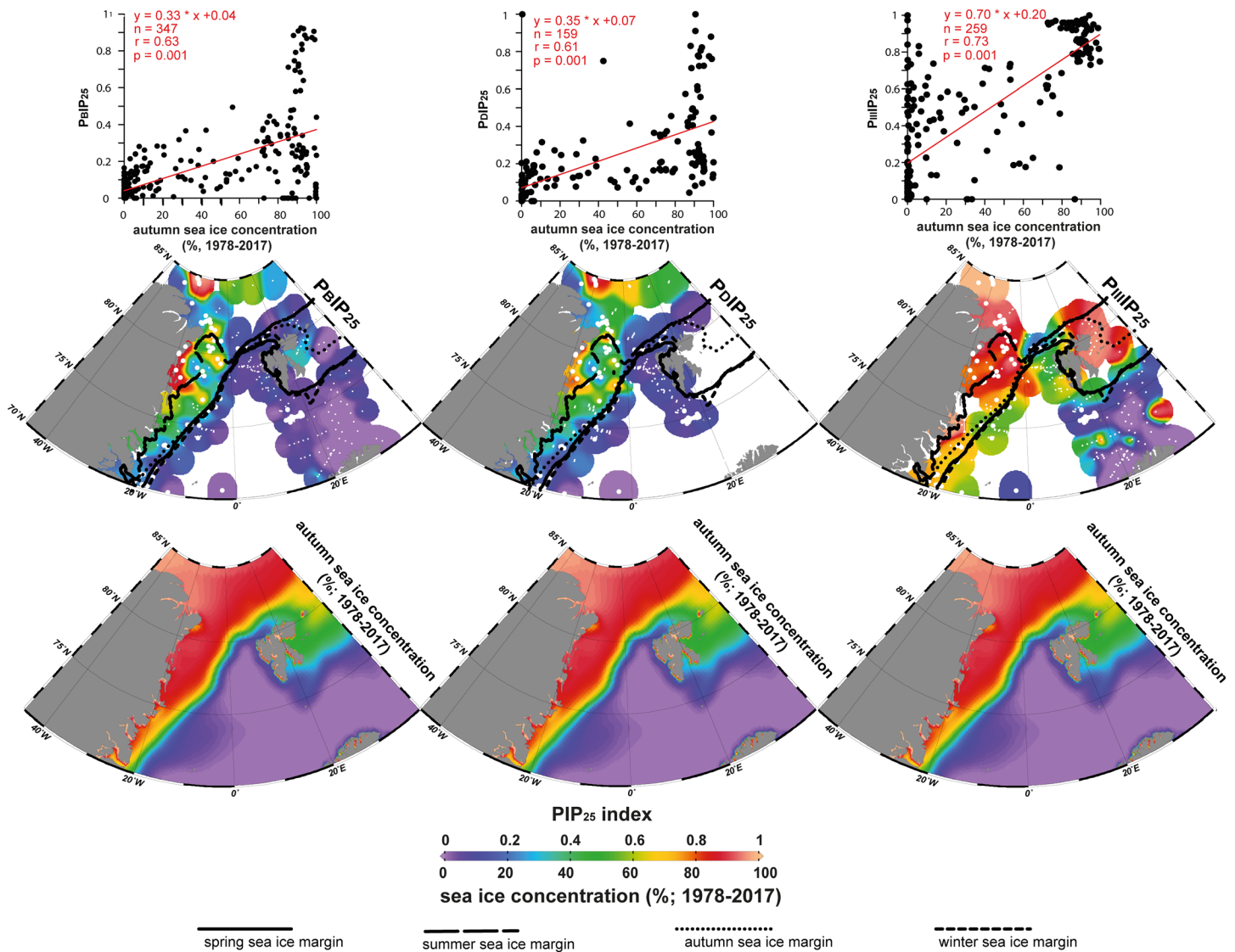| Season	P_BIP_{25}	P_DIP_{25}	$P_{III}IP_{25}$
Spring	0.52	0.56	0.67
Summer	0.52	0.58	0.63
Autumn	0.63	0.61	0.73
Winter	0.56	0.52	0.65

Figure 9. Comparison of sea ice reconstructions using P_BIP_{25}, P_DIP_{25}, and $P_{III}IP_{25}$ with the seasonal sea ice distribution in Fram Strait. The upper panels show correlations of the specific sea ice reconstruction to spring sea ice concentrations (Cavalieri et al., 1996, updated 2017). The middle panels show the spatial distribution of PIP_{25} indices; white points indicate location of surface samples. The seasonal ice margins are indicated by black lines: solid = spring (AMJ); wide dashed = summer (JAS); dotted = autumn (OND); narrow dashed = winter (JFM) (Cavalieri et al., 1996, updated 2017). Below the corresponding seasons with the highest correlations are shown (Cavalieri et al., 1996, updated 2017).

sea ice reconstructions. Some heterotrophic dinoflagellate cyst taxa have been shown to be common in sea ice environments (e.g., *Islandinium minutum, Islandinium? cezare,* and *Echinidinium karaense*), whereas many others develop only in sea ice-free settings (de Vernal, Gersonde, et al., 2013; de Vernal et al., 2001, 2008, 2020; Kunz-Pirrung, 2001; Matthiessen et al., 2005; Rochon et al., 1999). The dinoflagellate cyst *Polarella glacialis*, which is a photosynthetic species that blooms in sea ice brine channels and produces cysts (Stoecker et al., 1998), has been recorded both in Antarctic and Arctic sea ice (Matthiessen et al., 2005; Montresor et al., 2003). In the Northern Hemisphere, organic-walled cysts of *Polarella glacialis* have been reported to occur in sediments of many seasonally sea ice-covered environments such as the Hudson Bay (e.g., Heikkilä et al., 2014) and Greenland fjords (Ribeiro et al., 2017). It has been found with a similar distribution pattern as IP_{25} in Northeast Greenland Shelf sediments (Limoges et al., 2018). However, the cysts of *Polarella glacialis*, which are small and fragile, have in the past not been routinely recovered, making it difficult to use this species for quantitative data treatment in large-scale databases. Nevertheless, although the relationship between sea ice and the assemblages of dinoflagellate cysts preserved in the

sediment is indirect, the development of large standardized databases has permitted the use of MATs or transfer functions to estimate the seasonal extent of sea ice cover (de Vernal, Eynaud, et al., 2005; de Vernal, Gersonde, et al., 2013; de Vernal, Hillaire-Marcel, et al., 2005). The MAT approach has been applied to reconstruct sea ice during the Last Glacial Maximum and the Holocene at many sites of the Northern Hemisphere (e.g., de Vernal, Eynaud, et al., 2005; de Vernal, Rochon, et al., 2013).

The new comprehensive IP_{25}/PIP_{25} database encompasses an area comparable with the dinoflagellate cyst database ($n = 1,968$) generated by de Vernal et al. (2020) and de Vernal, Rochon, et al. (2013). The biomarker database is still considerably smaller (P_BIP_{25}: $n = 733$; P_DIP_{25}: $n = 489$; $P_{III}IP_{25}$: $n = 593$), and the indices used were not yet standardized on a hemispheric scale. Nevertheless, the spatial coverage north of 45°N is relatively similar, which provides a suitable foundation to compare biomarker and dinoflagellate cyst-based approaches for sea ice estimates.

Multivariate analyses performed on the most recent update of the dinoflagellate cyst database (de Vernal et al., 2020) indicate that the distribution of dinoflagellate cyst assemblages is explained by several environmental parameters. Among these is the mean annual sea ice concentration or the seasonal sea ice cover extent. The correlation coefficient between sea ice and the first axis that explains 36.7% of the variance is 0.65 (cf. de Vernal et al., 2020). None of the dinoflagellate cyst taxa recovered in sediments and compiled in the Northern Hemisphere database are exclusively related to sea ice. Hence, the overall relationship is indirect and rather linked to the association of species that characterize the respective lengths of the seasons with and without sea ice, which is proportional to the mean annual concentration. Estimating sea ice concentration in spring could be done but would be spurious, as it would rely on linearity between seasonal and mean annual sea ice concentrations.

The quantitative reconstruction of sea ice from dinoflagellate cysts assemblages has uncertainties that could be quantified from the correlation coefficient between observations and proxy-based estimates, expressed as root-mean-square error of prediction (RMSEP) obtained from a verification subset of data. With the application of the MAT to dinoflagellate cyst assemblages from the Northern Hemisphere, the RMSEP is about 12% of sea ice concentrations (cf. de Vernal, Rochon, et al., 2013). This metric of reliability may vary, however, depending on the technique used, and the regional calibration data set including the spatial autocorrelation of its sites (e.g., Bonnet et al., 2010; Guiot & de Vernal, 2011; Hohmann et al., 2019). The relatively large error of prediction of the sea ice concentration estimates with the PIP_{25} indices may be due to the smaller size of the biomarker data set and the low number of data points in year-round sea ice free regions. Hence, it may be expected that expanding the biomarker database toward year-round ice-free regions would improve the statistics by a wider range of environmental conditions, thus increasing the correlations between sea ice concentrations and IP_{25}-related indices.

For a more direct comparison between the dinoflagellate cyst and biomarker proxies, we use the P_BIP_{25} index, which is the index with the largest number of data points in the database ($n = 733$). In general, dinoflagellate cysts and IP_{25} proxies reflect important characteristics of modern sea ice in the marginal Arctic seas including Baffin Bay, Fram Strait, the Barents Sea, and the Bering Sea (Figure 10). Both proxies permit to distinguish between sea ice free, seasonal sea ice conditions, and multiyear sea ice. However, the sea ice signals of the two proxies differ in certain instances, which are in line with findings from the Canadian Arctic (Pieńkowski et al., 2017). In contrast to dinoflagellate cysts used for MAT, IP_{25} is produced by diatoms living inside sea ice. It indicates the occurrence of seasonal sea ice and may be used to reconstruct the MIZ or polynya conditions as shown by Belt et al. (2018, 2019). The abundance of IP_{25} relative to other biomarkers may even serve as a tracer of sea ice concentration in spring and/or autumn as illustrated here and elsewhere. Therefore, the combined use of dinoflagellate cysts and biomarker-based sea ice reconstruction, respectively, providing information on the number of month with and without sea ice cover and the concentrations of sea ice in spring and possibly late summer and autumn, will provide valuable insights on sea ice conditions and increase the accuracy of proxy reconstructions. Furthermore, the development of a Northern Hemisphere-wide diatom database and other proxies including ostracods, foraminifera, and ancient DNA signals, may contribute to more detailed regional sea ice reconstructions. Especially the large amount of diatom surface studies may provide a first proxy ideal to compare with existing biomarker and dinoflagellate databases, assuming that biogenic silica of diatoms is well preserved in sediments, as it is the case in North Atlantic and eastern Baffin Bay (Koç et al., 2019; Krawczyk et al., 2017; Sha et al., 2014).
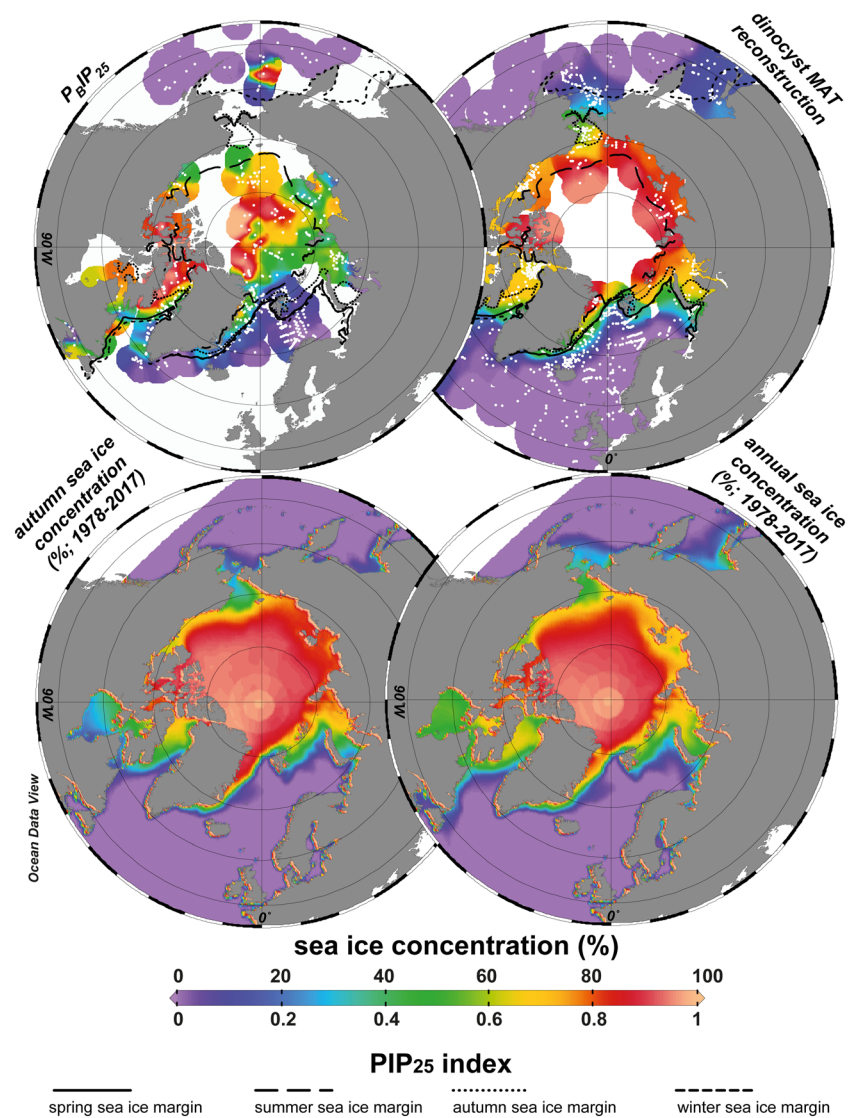
Figure 10. Sea-ice reconstructions based on the P_BIP_{25} sea ice index from the updated (sub-)Arctic database (this study; Belt et al., 2007, 2013, 2015; Méheust et al., 2013; Müller et al., 2011; Navarro-Rodriguez et al., 2013; Pieńkowski et al., 2017; Ribeiro et al., 2017; Smik et al., 2016; Xiao et al., 2013, 2015) and MAT dinoflagellate cyst database (mean annual concentration; de Vernal, Gersonde, et al., 2013) in the Northern Hemisphere. The seasonal ice margins are indicated by black lines: solid = spring (AMJ); wide dashed = summer (JAS); dotted = autumn (OND); narrow dashed = winter (JFM) (Cavalieri et al., 1996, updated 2017). The lower panel shows the autumn and annual sea ice concentration, the sea ice condition reflected by P_BIP_{25}, and dinoflagellate cyst reconstructions.

7. Conclusions

With the extended comprehensive data set that combines new and published surface sediment biomarker records, we can confirm the pan-Arctic applicability of the biomarker approach for sea ice reconstructions. The main conclusions are as follows:

1. On an Arctic-wide scale, all PIP_{25} indices show robust correlations not only with spring but also with autumn sea ice concentration, independent of the phytoplankton marker used for its calculation. In general, the c factor is one of the largest uncertainties when using all PIP_{25} indices for sea ice reconstructions.
2. On a regional scale, the PIP_{25} indices differ in their correlations to seasonal sea ice. In Baffin Bay, with strong spatial sea ice variability, the PIP_{25} indices probably reflect mostly spring and autumn sea ice. In Fram Strait, with lower spatial variability and inhibited phytoplankton productivity, the PIP_{25}

indices show less pronounced correlations to the different seasonal sea ice conditions. All PIP_{25} indices show the highest correlations to autumn sea ice concentrations, whereas the correlations to other seasons are also significant.

3. As the regional differences in the relationship between PIP_{25} indices and sea ice concentration may yield the possibility to reconstruct seasonal sea ice conditions, an approach combining dinoflagellate cyst (and diatom) assemblages and biomarkers may allow the quantification of seasonal sea ice concentration signals with a high level of confidence.

Data Availability Statement

All biomarker data presented in this study will be available under https://doi.pangaea.de/10.1594/PANGAEA.905494 upon publishing.

References

Aagaard, K., & Coachman, L. (1968a). The East Greenland Current north of Denmark Strait: Part I. *Arctic*, *21*(3), 181–200.

Aagaard, K., & Coachman, L. (1968b). The East Greenland Current north of Denmark Strait: Part II. *Arctic*, *21*(3), 267–290.

Aagaard-Sørensen, S., Husum, K., Hald, M., & Knies, J. (2010). Paleoceanographic development in the SW Barents Sea during the Late Weichselian-Early Holocene transition. *Quaternary Science Reviews*, *29*(25–26), 3442–3456. https://doi.org/10.1016/j.quascirev.2010.08.014

Andrews, J. T. (2009). Seeking a Holocene drift ice proxy: Non-clay mineral variations from the SW to N-central Iceland shelf: Trends, regime shifts, and periodicities. *Journal of Quaternary Science*, *24*(7), 664–676. https://doi.org/10.1002/jqs.1257

Andrews, J. T., Cabedo-Sanz, P., Jennings, A. E., Ólafsdóttir, S., Belt, S. T., & Geirsdóttir, Á. (2018). Sea ice, ice-rafting, and ocean climate across Denmark Strait during rapid deglaciation (16–12 cal ka BP) of the Iceland and East Greenland shelves. *Journal of Quaternary Science*, *33*, 112–130. https://doi.org/10.1002/jqs.3007

Andrews, J. T., & Syvitski, J. P. M. (1994). Sediment fluxes along the high latitude glaciated continental margins: Northeast Canada and Eastern Greenland. In *Material fluxes on the surface of the Earth*, *Board on Earth Sciences and Resources Commission on Geosciences, Environment, and Resources* (pp. 99–115). Washington, DC: National Research Council, National Academy Press.

Ardyna, M., Babin, M., Gosselin, M., Devred, E., Rainville, L., & Tremblay, J.-E. (2014). Recent Arctic Ocean sea ice loss triggers novel fall phytoplankton blooms. *Geophysical Research Letters*, *41*, 6207–6212. https://doi.org/10.1002/2014GL061047

Armand, L. K., & Leventer, A. (2010). Palaeo sea ice distribution and reconstruction derived from the geological record. In G. S. Thomas, & D. N. Dieckmann (Eds.), *Sea ice* (pp. 469–529). Oxford: Blackwell Publishing.

Årthun, M., Eldevik, T., Smedsrud, L. H., Skagseth, Ø., & Ingvaldsen, R. B. (2012). Quantifying the influence of Atlantic heat on Barents Sea ice variability and retreat. *Journal of Climate*, *25*(13), 4736–4743. https://doi.org/10.1175/JCLI-D-11-00466.1

Barrick, R. C., & Hedges, J. I. (1981). Hydrocarbon geochemistry of the Puget Sound region-II. Sedimentary diterpenoid, steroid and triterpenoid hydrocarbons. *Geochimica et Cosmochimica Acta*, *45*(3), 381–392. https://doi.org/10.1016/0016-7037(81)90247-7

Belt, S. T. (2018). Source-specific biomarkers as proxies for Arctic and Antarctic sea ice. *Organic Geochemistry*, *125*, 277–298. https://doi.org/10.1016/j.orggeochem.2018.10.002

Belt, S. T. (2019). What do IP_{25} and related biomarkers really reveal about sea ice change? *Quaternary Science Reviews*, *204*, 216–219. https://doi.org/10.1016/j.quascirev.2018.11.025

Belt, S. T., Brown, T. A., Ampel, L., Cabedo-Sanz, P., Fahl, K., Kocis, J. J., & Xu, Y. (2014). An inter-laboratory investigation of the Arctic sea ice biomarker proxy IP_{25} in marine sediments: Key outcomes and recommendations. *Climate of the Past*, *10*(1), 155–166. https://doi.org/10.5194/cp-10-155-2014

Belt, S. T., Brown, T. A., Ringrose, A. E., Cabedo-Sanz, P., Mundy, C. J., Gosselin, M., & Poulin, M. (2013). Quantitative measurement of the sea ice diatom biomarker IP_{25} and sterols in Arctic sea ice and underlying sediments: Further considerations for palaeo sea ice reconstruction. *Organic Geochemistry*, *62*, 33–45. https://doi.org/10.1016/j.orggeochem.2013.07.002

Belt, S. T., Brown, T. A., Smik, L., Assmy, P., & Mundy, C. J. (2018). Sterol identification in floating Arctic sea ice algal aggregates and the Antarctic sea ice diatom Berkeleya adeliensis. *Organic Geochemistry*, *118*, 1–3. https://doi.org/10.1016/j.orggeochem.2018.01.008

Belt, S. T., Brown, T. A., Smik, L., Tatarek, A., Wiktor, J., Stowasser, G., & Husum, K. (2017). Identification of C_{25} highly branched isoprenoid (HBI) alkenes in diatoms of the genus Rhizosolenia in polar and sub-polar marine phytoplankton. *Organic Geochemistry*, *110*, 65–72. https://doi.org/10.1016/j.orggeochem.2017.05.007

Belt, S. T., Cabedo-Sanz, P., Smik, L., Navarro-Rodriguez, A., Berben, S. M. P., Knies, J., & Husum, K. (2015). Identification of paleo Arctic winter sea ice limits and the marginal ice zone: Optimised biomarker-based reconstructions of late Quaternary Arctic sea ice. *Earth and Planetary Science Letters*, *431*, 127–139. https://doi.org/10.1016/j.epsl.2015.09.020

Belt, S. T., Massé, G., Rowland, S. J., Poulin, M., Michel, C., & LeBlanc, B. (2007). A novel chemical fossil of palaeo sea ice: IP25. *Organic Geochemistry*, *38*(1), 16–27. https://doi.org/10.1016/j.orggeochem.2006.09.013

Belt, S. T., & Müller, J. (2013). The Arctic sea ice biomarker IP_{25}: A review of current understanding, recommendations for future research and applications in palaeo sea ice reconstructions. *Quaternary Science Reviews*, *79*, 9–25. https://doi.org/10.1016/j.quascirev.2012.12.001

Belt, S. T., Smik, L., Brown, T. A., Kim, J.-H., Rowland, S. J., Allen, C. S., et al. (2016). Source identification and distribution reveals the potential of the geochemical Antarctic sea ice proxy $IPSO_{25}$. *Nature Communications*, *7*, 12655. https://doi.org/10.1038/ncomms12655

Belt, S. T., Smik, L., Köseoglu, D., Knies, J., & Husum, K. (2019). A novel biomarker-based proxy for the spring phytoplankton bloom in Arctic and sub-arctic settings—HBI T_{25}. *Earth and Planetary Science Letters*, *523*, 115703. https://doi.org/10.1016/j.epsl.2019.06.038

Bi, H., Zhang, Z., Wang, Y., Xu, X., Liang, Y., Huang, J., & Fu, M. (2019). Baffin Bay sea ice inflow and outflow: 1978–1979 to 2016–2017. *The Cryosphere*, *13*(3), 1025–1042. https://doi.org/10.5194/tc-13-1025-2019

Bonnet, S., de Vernal, A., Hillaire-Marcel, C., Radi, T., & Husum, K. (2010). Variability of sea-surface temperature and sea-ice cover in the Fram Strait over the last two millennia. *Marine Micropaleontology*, *74*(3–4), 59–74. https://doi.org/10.1016/j.marmicro.2009.12.001

Brown, T. A., Belt, S. T., Tatarek, A., & Mundy, C. J. (2014). Source identification of the Arctic sea ice proxy IP$_{25}$. *Nature Communications*, *5*, 4197. https://doi.org/10.1038/ncomms5197

Cabedo Sanz, P., Smik, L., & Belt, S. T. (2016). On the stability of various highly branched isoprenoid (HBI) lipids in stored sediments and sediment extracts. *Organic Geochemistry*, *97*, 74–77. https://doi.org/10.1016/j.orggeochem.2016.04.010

Cabedo-Sanz, P., Belt, S. T., Knies, J., & Husum, K. (2013). Identification of contrasting seasonal sea ice conditions during the Younger Dryas. *Quaternary Science Reviews*, *79*, 74–86. https://doi.org/10.1016/j.quascirev.2012.10.028

Campbell, D. C. (2013). *CCGS Hudson Expedition 2013-029 geological hazard assessment of Baffin Bay and biodiversity assessment of Hatton Basin* (Geological Survey of Canada, Open File 7594, pp. 1–124). https://doi.org/10.4095/293694

Campbell, D.C., & de Vernal, A. (2009). *Marine geology and paleoceanography of Baffin Bay and adjacent areas: Nain, NL to Halifax, NS: August 28–September 23, 2008*. Geological Survey of Canada.

Cavalieri, D. J., Parkinson, C. L., Gloersen, P., & Zwally, H. J. (1996). Sea ice concentrations from Nimbus-7 SMMR and DMSP SSM/I-SSMIS Passive Microwave Data, Version 1. Boulder, CO: NASA National Snow and Ice Data Center Distributed Active Archive Center. https://doi.org/10.5067/8GQ8LZQVL0VL

Chalut, K., & Merzouk, A. (2014). 2014 Expedition Report CCGS Amundsen. ArcticNet – AmundsenScience Program http://www.arctic-net.ulaval.ca/research/expedition2014.php

Comiso, J. C., Parkinson, C. L., Gersten, R., & Stock, L. (2008). Accelerated decline in the Arctic sea ice cover. *Geophysical Research Letters*, *35*, L01703. https://doi.org/10.1029/2007gl031972

Comiso, J. C., Cavalieri, D. J., Parkinson, C. L., & Gloersen, P. (1997). Passive microwave algorithms for sea ice concentration: A comparison of two techniques. *Remote Sensing of Environment*, *60*(3), 357–384. https://doi.org/10.1016/S0034-4257(96)00220-9

Cronin, T. M., Gemery, L., Briggs, W. M., Jakobsson, M., Polyak, L., & Brouwers, E. M. (2010). Quaternary sea-ice history in the Arctic Ocean based on a new Ostracode sea-ice proxy. *Quaternary Science Reviews*, *29*(25–26), 3415–3429. https://doi.org/10.1016/j.quascirev.2010.05.024

Cuny, J., Rhines, P. B., & Kwok, R. (2005). Davis Strait volume, freshwater and heat fluxes. *Deep-Sea Research Part I: Oceanographic Research Papers*, *52*(3), 519–542. https://doi.org/10.1016/j.dsr.2004.10.006

Damm, V. (Ed.) (2019). The Expedition PS115/1 of the Research Vessel POLARSTERN to the Greenland Sea and Wandel Sea in 2018. *Berichte zur Polar- und Meeresforschung = Reports on Polar and Marine Research, 727*, 186.

De Schepper, S., Ray, J. L., Skaar, K. S., Sadatzki, H., Ijaz, U. Z., Stein, R., & Larsen, A. (2019). The potential of sedimentary ancient DNA for reconstructing past sea ice evolution. *The ISME Journal*, *13*(10), 2566–2577. https://doi.org/10.1038/s41396-019-0457-1

de Vernal, A., Eynaud, F., Henry, M., Hillaire-Marcel, C., Londeix, L., Mangin, S., et al. (2005). Reconstruction of sea-surface conditions at middle to high latitudes of the Northern Hemisphere during the Last Glacial Maximum (LGM) based on dinoflagellate cyst assemblages. *Quaternary Science Reviews*, *24*, 897–924. https://doi.org/10.1016/j.quascirev.2004.06.014

de Vernal, A., Gersonde, R., Goosse, H., Seidenkrantz, M. S., & Wolff, E. W. (2013). Sea ice in the paleoclimate system: The challenge of reconstructing sea ice from proxies—An introduction. *Quaternary Science Reviews*, *79*, 1–8. https://doi.org/10.1016/j.quascirev.2013.08.009

de Vernal, A., Henry, M., Matthiessen, J., Mudie, P. J., Rochon, A., Boessenkool, K. P., & Voronina, E. (2001). Dinoflagellate cyst assemblages as tracers of sea-surface conditions in the northern North Atlantic, Arctic and sub-Arctic seas: The new '$n = 677$' data base and its application for quantitative palaeoceanographic reconstruction. *Journal of Quaternary Science*, *16*(7), 681–698. https://doi.org/10.1002/jqs.659

de Vernal, A., Hillaire-Marcel, C., & Darby, D. A. (2005). Variability of sea ice cover in the Chukchi Sea (western Arctic Ocean) during the Holocene. *Paleoceanography*, *20*, PA4018. https://doi.org/10.1029/2005PA001157

de Vernal, A., Hillaire-Marcel, C., Solignac, S., Radi, T., & Rochon, A. (2008). Reconstructing sea-ice conditions in the Arctic and subarctic prior to human observations. In E. Weaver (Ed.), *Arctic sea ice decline: Observations, projections, mechanisms, and implications*, *Monograph* (pp. 27–45). Washington, DC: American Geophysical Union.

de Vernal, A., Radi, T., Zaragosi, S., Van Nieuwenhove, N., Rochon, A., Allan, E., et al. (2020). Distribution of common modern dinoflagellate cyst taxa in surface sediments of the Northern Hemisphere in relation to environmental parameters: The new $n=1968$ database. *Marine Micropaleontology*, *159*, 101796. https://doi.org/10.1016/j.marmicro.2019.101796

de Vernal, A., Rochon, A., Fréchette, B., Henry, M., Radi, T., & Solignac, S. (2013). Reconstructing past sea ice cover of the Northern Hemisphere from dinocyst assemblages: Status of the approach. *Quaternary Science Reviews*, *79*, 122–134. https://doi.org/10.1016/j.quascirev.2013.06.022

Dieckmann, G. N., & Hellmer, H. (2008). The importance of sea ice: An overview. In D. N. Thomas, & G. S. Dieckmann (Eds.), *Sea ice: An introduction to its physics, chemistry biology, and geology* (pp. 1–21). Oxford: Blackwell Science.

Dorschel, B., Afanasyeva, V., Bender, M., Dreutter, S., Eisermann, H., Gebhardt, C., et al. (2016). BAFFEAST past Greenland Ice Sheet dynamics, Palaeoceanography and Plankton Ecology in the Northeast Baffin Bay. MARIA S. MERIAN-Berichte. Retrieved from https://www.ldf.uni-hamburg.de/merian/wochenberichte/wochenberichte-merian/msm44-msm46/msm44-scr.pdf

Dorschel, B., Allan, E., Bartels, M. Campbell, C., Couette, P.-O., Diekamp, V., et al. (2017). Maria S. Merian Berichte WESTBAFF reconstruction of the Laurentide ice sheet drainage into the northwest Baffin Bay and the palaeoceanography of the west Baffin Bay Cruise No. MSM66 22nd of July 2017–28th of August 2017, Nuuk (Greenland)-Reykjavik (Iceland)

Drinkwater, K. F. (1996). Atmospheric and oceanic variability in the northwest Atlantic during the 1980s and early 1990s. *Journal of Northwest Atlantic Fishery Science*, *18*, 77–97. https://doi.org/10.2960/J.v18.a6

Fahl, K., & Stein, R. (1997). Modern organic carbon deposition in the Laptev Sea and the adjacent continental slope: Surface water productivity vs. terrigenous input. *Organic Geochemistry*, *26*(5–6), 379–390. https://doi.org/10.1016/S0146-6380(97)00007-7

Fahl, K., & Stein, R. (1999). Biomarkers as organic-carbon-source and environmental indicators in the late quaternary Arctic Ocean: Problems and perspectives. *Marine Chemistry*, *63*(3–4), 293–309. https://doi.org/10.1016/S0304-4203(98)00068-1

Fahl, K., & Stein, R. (2012). Modern seasonal variability and deglacial/Holocene change of central Arctic Ocean sea-ice cover: New insights from biomarker proxy records. *Earth and Planetary Science Letters*, *351–352*, 123–133. https://doi.org/10.1016/j.epsl.2012.07.009

Fahl, K., Stein, R., Gaye-Haake, B., Gebhardt, C., Kodina, L. A., Unger, D., & Ittekkot, V. (2003). Biomarkers in surface sediments from Ob and Yenisei estuaries and southern Kara Sea: Evidence for particulate organic carbon sources, pathways, and degradation. In R. Stein, K. Fahl, D. K. Fütterer, E. M. Galimov, & O. V. Stepanets (Eds.), *Siberian river run-off in the Kara Sea: Characterisation, quantification, variability, and environmental significance, Proceedings in marine sciences* (Vol. 6, pp. 329–348). Amsterdam: Elsevier.

Fetterer, F., Knowles, K., Meier, W. N., Savoie, M., & Windnagel, A. K. (2017). *Sea Ice Index, Version 3*. Boulder, CO: National Snow and Ice Data Center (NSIDC).

GEBCO. (n.d.). General Bathymetric Chart of the Oceans. Retrieved from http://www.gebco.net

Geissler, W. (2013). Maria S. Merian; Cruise No. MSM 31 Tromsø—Bremen Short cruise description Cruise Rep. Maria S. Merian Cruise No. MSM 31 1–18.

Gloersen, P., Campbell, W. J., Cavalieri, D. J., Comiso, J. C., Parkinson, C. L., & Zwally, H. J. (1993). Satellite passive microwave observations and analysis of Arctic and Antarctic sea ice, 1978–1987. *Annals of Glaciology*, *17*, 149–154. https://doi.org/10.1016/0021-9169(95)90010-1

Goad, L. J., & Withers, N. (1982). Identification of 27-nor-(24R)-24-methylcholesta-5,22-dien-3β-ol and brassicasterol as the major sterols of the marine dinoflagellate *Gymnodinium* simplex. *Lipids*, *17*(12), 853–858. https://doi.org/10.1007/BF02534578

Gosselin, M., Levasseur, M., Wheeler, P. A., Horner, R. A., & Booth, B. C. (1997). New measurements of phytoplankton and ice algal production in the Arctic Ocean. *Deep-Sea Research Part II: Topical Studies in Oceanography*, *44*(8), 1623–1644. https://doi.org/10.1016/S0967-0645(97)00054-4

Guiot, J., & de Vernal, A. (2011). is spatial autocorrelation introducing biases in the apparent accuracy of paleoclimatic reconstructions? *Quaternary Science Reviews*, *30*(15–16), 1965–1972. https://doi.org/10.1016/j.quascirev.2011.04.022

Hanebuth, T. (2009). *Short Cruise Report: RV Maria S. Merian Cruise MSM 30. Short Cruise Report*. Retrieved from https://www.ldf.uni-hamburg.de/merian/wochenberichte/wochenberichtemerian/msm29-msm31/msm30-scr.pdf

He, D., Simoneit, B. R. T., Xu, Y., & Jaffé, R. (2016). Occurrence of unsaturated C_{25} highly branched isoprenoids (HBIs) in a freshwater wetland. *Organic Geochemistry*, *93*, 59–67. https://doi.org/10.1016/j.orggeochem.2016.01.006

Heikkilä, M., Pospelova, V., Hochheim, K. P., Kuzyk, Z. Z. A., Stern, G. A., Barber, D. G., & Macdonald, R. W. (2014). Surface sediment dinoflagellate cysts from the Hudson Bay system and their relation to freshwater and nutrient cycling. *Marine Micropaleontology*, *106*, 79–109. https://doi.org/10.1016/j.marmicro.2013.12.002

Hirche, H. J., Baumann, M. E. M., Kattner, G., & Gradinger, R. (1991). Plankton distribution and the impact of copepod grazing on primary production in Fram Strait, Greenland Sea. *Journal of Marine Systems*, *2*(3–4), 477–494. https://doi.org/10.1016/0924-7963(91)90048-Y

Hoff, U., Rasmussen, T. L., Stein, R., Ezat, M. E., & Fahl, K. (2016). Sea ice and millennial-scale climate variability in the Nordic seas 90 kyr ago to present. *Nature Communications*, *7*, 12247. https://doi.org/10.1038/ncomms12247

Hohmann, S., Kucera, M., & de Vernal, A. (2019). Identifying the signature of surface-ocean properties in dinocyst assemblages: Implications for quantitative paleoceanographical reconstructions by transfer functions and analogue techniques. *Marine Micropaleontology*, 101796. https://doi.org/10.1016/j.marmicro.2019.101796

Hopkins, T. S. (1991). The GIN Sea—A synthesis of its physical oceanography and literature review 1972-1985. *Earth Science Reviews*, *30*(3–4), 175–318. https://doi.org/10.1016/0012-8252(91)90001-V

Hörner, T., Stein, R., Fahl, K., & Birgel, D. (2016). Post-glacial variability of sea ice cover, river run-off and biological production in the western Laptev Sea (Arctic Ocean)—A high-resolution biomarker study. *Quaternary Science Reviews*, *143*, 133–149. https://doi.org/10.1016/j.quascirev.2016.04.011

Humlum, O. (1985). The glaciation level in West Greenland. *Arctic and Alpine Research*, *17*(3), 311–319. https://doi.org/10.1080/00040851.1985.12004038

Jakobsson, M., Mayer, L. A., Coakley, B., Dowdeswell, J. A., Forbes, S., Fridman, B., et al. (2012). The International Bathymetric Chart of the Arctic Ocean (IBCAO) Version 3.0. *Geophysical Research Letters*, *39*, L12609. https://doi.org/10.1029/2012gl052219

Jensen, L.M., & Christensen, T.R. (2014). Nuuk ecological research operations, 7th annual report. Aarhus Univ. DCE—Danish Cent. Environ. Energy 94 pp.

Johannessen, O. M., Shalina, E. V., & Miles, M. W. (1999). Satellite evidence for an Arctic sea ice cover in transformation. *Science*, *286*(5446), 1937–1939. https://doi.org/10.1126/science.286.5446.1937

Kanazwa, A., Yoshioka, M., & Teshima, S. I. (1971). Occurence of Brassicasteril in diatoms, *Cyclotella-Nana* and *Nitzschia-Closterium*. *Bulletin of the Japanese Society of Scientific Fisheries*, *37*(9), 899–903. https://doi.org/10.2331/suisan.37.899

Kanzow, T. (Ed.) (2018) The Expedition PS109 of the research vessel POLARSTERN to the Nordic Seas in 2017. Berichte zur Polar- und Meeresforschung https://doi.org/10.2312/BzPM_0715_2018

Knies, J., Cabedo-Sanz, P., & Belt, S. T. (2014). The emergence of modern sea ice cover in the Arctic Ocean. *Nature Communications*, *5*, 5608. https://doi.org/10.1038/ncomms6608

Knies, J., Pathirana, I., Cabedo-Sanz, P., Banica, A., Fabian, K., Rasmussen, T. L., & Belt, S. T. (2017). Sea-ice dynamics in an Arctic coastal polynya during the past 6500 years. *Arktos*, *3*, 1. https://doi.org/10.1007/s41063-016-0027-y

Koç, N., Jansen, E., & Haflidason, H. (1993). Paleoceanographic reconstructions of surface ocean conditions in the Greenland, Iceland and Norwegian seas through the last 14 ka based on diatoms. *Quaternary Science Reviews*, *12*(2), 115–140. https://doi.org/10.1016/0277-3791(93)90012-B

Koç, N., Miettinen, A., Divine, D., Husum, K., & Divina, S. (2019). Inventory of marine planktic diatom slides from a network of marine sediment cores and surface sediment samples stored in the Norwegian Polar Institute. [data set]. Norwegian Polar Institute. https://doi.org/10.21334/npolar.2019.d2325358

Köseoğlu, D., Belt, S. T., Smik, L., Yao, H., Panieri, G., & Knies, J. (2018). Complementary biomarker-based methods for characterising Arctic sea ice conditions: A case study comparison between multivariate analysis and the PIP25 index. *Geochimica et Cosmochimica Acta*, *222*, 406–420. https://doi.org/10.1016/j.gca.2017.11.001

Krawczyk, D., Witkowski, A., Juul-Pedersen, T., Arendt, K. E., Mortensen, J., & Rysgaard, S. (2015). Microplankton succession in a SW Greenland tidewater glacial fjord influenced by coastal inflows and run-off from the Greenland Ice Sheet. *Polar Biology*, *38*, 1515–1533. https://doi.org/10.1007/s00300-015-1715-y

Krawczyk, D. W., Witkowski, A., Moros, M., Lloyd, J. M., Høyer, J. L., Miettinen, A., & Kuijpers, A. (2017). Quantitative reconstruction of Holocene sea ice and sea surface temperature off West Greenland from the first regional diatom data set. *Paleoceanography*, *32*, 18–40. https://doi.org/10.1002/2016PA003003

Kristoffersen, Y., & Tholfsen, A. (2016). Ice drift station FRAM-2014/2015 weekly reports. NERSC technical reports no. 365, Nansen environmental and remote sensing Center, Bergen, Norway (p. 333).

Kunz-Pirrung, M. (2001). Dinoflagellate cyst assemblages in surface sediments of the Laptev Sea region (Arctic Ocean) and their relationship to hydrographic conditions. *Journal of Quaternary Science: Published for the Quaternary Research Association*, *16*(7), 637–649. https://doi.org/10.1002/jqs.647

Kvingedal, B. (2005). Sea-ice extent and variability in the Nordic Seas, 1967–2002. In H. Drange, T. Dokken, T. Furevik, R. Gerdes, & W. Berger (Eds.), *The Nordic Seas: An integrated perspective*, *Geophysical Monograph* (Vol. 158, pp. 39–49). Washington, DC: American Geophysical Union.

Lamping, N., Müller, J., Esper, O., Hillenbrand, C.-D., Smith, J. A., & Kuhn, G. (2020). Highly branched isoprenoids reveal onset of deglaciation followed by dynamic sea-ice conditions in the western Amundsen Sea, Antarctica. *Quaternary Science Reviews*, *228*, 106103. https://doi.org/10.1016/j.quascirev.2019.106103

Limoges, A., Ribeiro, S., Weckström, K., Heikkilä, M., Zamelczyk, K., Andersen, T. J., & Seidenkrantz, M. S. (2018). Linking the modern distribution of biogenic proxies in high Arctic Greenland shelf sediments to sea ice, primary production, and Arctic-Atlantic inflow. *Journal of Geophysical Research: Biogeosciences*, *123*, 760–786. https://doi.org/10.1002/2017JG003840

Loeng, H. (1991). Features of the physical oceanographic conditions of the Barents Sea. *Polar Research*, *10*(1), 5–18. https://doi.org/10.3402/polar.v10i1.6723

Macdonald, R.W., Harner, T., Fyfe, J., Loeng, H., & Weingartner, T. (2003). AMAP Assessment 2002: The influence of global change on contaminant pathways to, within, and from the Arctic, Arctic Monitoring and Assessment Programme (AMAP).

Martin, T., & Wadhams, P. (1999). Sea-ice flux in the East Greenland Current. *Deep Sea Research Part II: Topical Studies in Oceanography*, *46*(6–7), 1063–1082. https://doi.org/10.1016/S0967-0645(99)00016-8

Massé, G., Belt, S. T., Crosta, X., Schmidt, S., Snape, I., Thomas, D. N., & Rowland, S. J. (2011). Highly branched isoprenoids as proxies for variable sea ice conditions in the Southern Ocean. *Antarctic Science*, *23*(5), 487–498. https://doi.org/10.1017/S0954102011000381

Matthiessen, J., de Vernal, A., Head, M., Okolodkov, Y., Zonneveld, K., & Harland, R. (2005). Modern organic-walled dinoflagellate cysts in Arctic marine environments and their (paleo-) environmental significance. *Paläontologische Zeitschrift*, *79*(1), 3–51. https://doi.org/10.1007/BF03021752

Matthiessen, J., Schreck, M., de Schepper, S., Zorzi, C., & de Vernal, A. (2018). Quaternary dinoflagellate cysts in the Arctic Ocean: Potential and limitations for stratigraphy and paleoenvironmental reconstructions. *Quaternary Science Reviews*, *192*, 1–26. https://doi.org/10.1016/j.quascirev.2017.12.020

Méheust, M., Fahl, K., & Stein, R. (2013). Variability in modern sea surface temperature, sea ice and terrigenous input in the sub-polar North Pacific and Bering Sea: Reconstruction from biomarker data. *Organic Geochemistry*, *57*, 54–64. https://doi.org/10.1016/j.orggeochem.2013.01.008

Meyers, P. A. (1997). Organic geochemical proxies of paleoceanographic, paleolimnologic, and paleoclimatic processes. *Organic Geochemistry*, *27*(5–6), 213–250. https://doi.org/10.1016/S0146-6380(97)00049-1

Michel, C., Hamilton, J., Hansen, E., Barber, D., Reigstad, M., Iacozza, J., et al. (2015). Arctic Ocean outflow shelves in the changing Arctic: A review and perspectives. *Progress in Oceanography*, *139*, 66–88. https://doi.org/10.1016/j.pocean.2015.08.007

Mienert, J., Andrews, J. T., & Milliman, J. D. (1992). The East Greenland continental margin (65°N) since the last deglaciation: Changes in seafloor properties and ocean circulation. *Marine Geology*, *106*, 217–238. https://doi.org/10.1016/0025-3227(92)90131-Z

Miettinen, A., Divine, D., Husum, K., Koç, N., & Jennings, A. (2015). Exceptional ocean surface conditions on the SE Greenland shelf during the Medieval Climate Anomaly. *Paleoceanography*, *30*, 1657–1674. https://doi.org/10.1002/2015PA002849

MODIS (n.d.). Moderate Resolution Imaging Spectroradiomater, NASA Chlorophyll A:_https://oceandata.sci.gsfc.nasa.gov/MODISAqua/Mapped/Seasonal/4km/chlor_a Productivity: https://modis.gsfc.nasa.gov/data/dataprod

Montresor, M., Lovejoy, C., Orsini, L., Procaccini, G., & Roy, S. (2003). Bipolar distribution of the cyst-forming dinoflagellate Polarella glacialis. *Polar Biology*, *26*(3), 186–194. https://doi.org/10.1007/s00300-002-0473-9

Müller, J., Massé, G., Stein, R., & Belt, S. T. (2009). Variability of sea-ice conditions in the Fram Strait over the past 30,000 years. *Nature Geoscience*, *2*(11), 772–776. https://doi.org/10.1038/ngeo665

Müller, J., & Stein, R. (2014). High-resolution record of late glacial and deglacial sea ice changes in Fram Strait corroborates ice-ocean interactions during abrupt climate shifts. *Earth and Planetary Science Letters*, *403*, 446–455. https://doi.org/10.1016/j.epsl.2014.07.016

Müller, J., Wagner, A., Fahl, K., Stein, R., Prange, M., & Lohmann, G. (2011). Towards quantitative sea ice reconstructions in the northern North Atlantic: A combined biomarker and numerical modelling approach. *Earth and Planetary Science Letters*, *306*(3–4), 137–148. https://doi.org/10.1016/j.epsl.2011.04.011

Myers, P., Kulan, N., & Ribergaard, M. (2007). Irminger Water variability in the West Greenland Current. *Geophysical Research Letters*, *34*, L17601. https://doi.org/10.1029/2007GL030419

Nam, S.-I., Stein, R., Grobe, H., & Hubberten, H. (1995). Later-Quaternary glacial-interglacial changes in sediment composition at the East Greenland continental margin and their paleooceanographic implications. *Marine Geology*, *122*(3), 243–262. https://doi.org/10.1016/0025-3227(94)00070-2

Navarro-Rodriguez, A., Belt, S. T., Knies, J., & Brown, T. A. (2013). Mapping recent sea ice conditions in the Barents Sea using the proxy biomarker IP$_{25}$: Implications for palaeo sea ice reconstructions. *Quaternary Science Reviews*, *79*, 26–39. https://doi.org/10.1016/j.quascirev.2012.11.025

Notz, D., & Stroeve, J. (2016). Observed Arctic sea-ice loss directly follows anthropogenic CO_2 emission. *Science*, *354*(6313), 747–750. https://doi.org/10.1126/science.aag2345

Notz, D., & Stroeve, J. (2018). The trajectory towards a seasonally-ice-free Arctic Ocean. *Current Climate Change Reports*, *4*(4), 407–416. https://doi.org/10.1007/s40641-018-0113-2

NSIDC. (n.d.). National Snow and Ice Data Base. Retrieved from http://nsidc.org/data/G10010

Oregon State University (n.d.). http://orca.science.oregonstate.edu/2160.by.4320.monthly.xyz.vgpm.m.chl.m.sst.php

Parkinson, C. L. (2008). Satellite passive-microwave measurements of sea ice. In K. K. Steele, H. J. Thorpe, & A. S. Turekian (Eds.), *Encyclopedia of ocean sciences* (2nd ed. pp. 80–90). Oxford: Academic Press. https://doi.org/10.1016/B978-012374473-9.00805-5

Perner, K., Moros, M., Lloyd, J. M., Jansen, E., & Stein, R. (2015). Mid to late Holocene strengthening of the East Greenland Current linked to warm subsurface Atlantic water. *Quaternary Science Reviews*, *129*, 296–307. https://doi.org/10.1016/j.quascirev.2015.10.007

Perovich, D. K., Grenfell, T. C., Light, B., Elder, B. C., Harbeck, J., Polashenski, C., & Stelmach, C. (2009). Transpolar observations of the morphological properties of Arctic sea ice. *Journal of Geophysical Research*, *114*, C00A04. https://doi.org/10.1029/2008JC004892

Petrich, C., & Eicken, H. (2010). Growth, structure and properties of sea ice. In G. S. Thomas, & D. N. Dieckmann (Eds.), *Sea Ice* (pp. 23–78). Oxford, UK: Wiley-Blackwell. https://doi.org/10.1002/9781444317145.ch2

Pieńkowski, A. J., Gill, N. K., Furze, M. F. A., Mugo, S. M., Marret, F., & Perreaux, A. (2017). Arctic sea-ice proxies: Comparisons between biogeochemical and micropalaeontological reconstructions in a sediment archive from Arctic Canada. *Holocene*, *27*(5), 665–682. https://doi.org/10.1177/0959683616670466

Pollehne, F. (2015) Short Cruise Report MARIA S. MERIAN MSM 46 Halifax - 25.08.2015 St. John's – 26.09.2015

Popova, E. E., Yool, A., Coward, A. C., Aksenov, Y. K., Alderson, S. G., de Cuevas, B. A., & Anderson, T. R. (2010). Control of primary production in the Arctic by nutrients and light: insights from a high resolution ocean general circulation model. *Biogeosciences Discuss*, *7*, 5557–5620. https://doi.org/10.5194/bgd-7-5557-2010

Ribeiro, S., Moros, M., Ellegaard, M., & Kuijpers, A. (2012). Climate variability in West Greenland during the past 1500 years: Evidence from a high-resolution marine palynological record from Disko Bay. *Boreas*, *41*(1), 68–83. https://doi.org/10.1111/j.1502-3885.2011.00216.x

Ribeiro, S., Sejr, M. K., Limoges, A., Heikkilä, M., Andersen, T. J., Tallberg, P., et al. (2017). Sea ice and primary production proxies in surface sediments from a High Arctic Greenland fjord: Spatial distribution and implications for palaeoenvironmental studies. *Ambio*, *46*(S1), 106–118. https://doi.org/10.1007/s13280-016-0894-2

Rochon, A., Vernal, A. D., Turon, J. L., Matthießen, J., & Head, M. J. (1999). Distribution of recent dinoflagellate cysts in surface sediments from the North Atlantic Ocean and adjacent seas in relation to sea-surface parameters. *American Association of Stratigraphic Palynologists Contribution Series*, *35*, 1–146.

Rowland, S. J., Allard, W. G., Belt, S. T., Massé, G., Robert, J. M., Blackburn, S., & Volkman, J. K. (2001). Factors influencing the distributions of polyunsaturated terpenoids in the diatom, Rhizosolenia setigera. *Phytochemistry*, *58*(5), 717–728. https://doi.org/10.1016/S0031-9422(01)00318-1

Rudels, B., Björk, G., Nilsson, J., Winsor, P., Lake, I., & Nohr, C. (2005). The interaction between waters from the Arctic Ocean and the Nordic Seas north of Fram Strait and along the East Greenland Current: Results from the Arctic Ocean-02 Oden expedition. *Journal of Marine Systems*, *55*(1–2), 1–30. https://doi.org/10.1016/j.jmarsys.2004.06.008

Sakshaug, E., Johnsen, G., Kristiansen, S., von Quillfeldt, C., Rey, F., Slagstad, D., & Thingstad, F. (2009). Phytoplankton and primary production. In E. Sakshaug, G. Johnsen, & K. Kovacs (Eds.), *Ecosystem Barents Sea* (pp. 167–208). Trondheim: Tapir Academic Press.

Schiltzer, R. (2017). Ocean Data View.

Schlitzer, R. (2019). Ocean Data View user's guide https://odv.awi.de

Schneider, W., & Budéus, G. (1997). Summary of the Northeast Water polynya formation and development (Greenland Sea). *Journal of Marine Systems*, *10*(1–4), 107–122. https://doi.org/10.1016/S0924-7963(96)00075-9

Seidenkrantz, M. S. (2013). Benthic foraminifera as palaeo sea-ice indicators in the subarctic realm—Examples from the Labrador Sea-Baffin Bay region. *Quaternary Science Reviews*, *79*, 135–144. https://doi.org/10.1016/j.quascirev.2013.03.014

Sha, L., Jiang, H., Seidenkrantz, M.-S., Knudsen, K. L., Olsen, J., Kuijpers, A., & Liu, Y. (2014). A diatom-based sea-ice reconstruction for the Vaigat Strait (Disko Bugt, West Greenland) over the last 5000 yr. *Palaeogeography, Palaeoclimatology, Palaeoecology*, *403*, 66–79. https://doi.org/10.1016/j.palaeo.2014.03.028

Simon, Q., Thouveny, N., Bourles, S. L., Nuttin, L., Hillaire-Marcel, C., & St-Onge, G. (2016). Authigenic ^{10}B/^{9}Be rations and ^{10}Be-fluxes (^{230}Thx-normalized) in central Baffin Bay sediments during the last glacial cycle: Paleoenvironmental implications. *Quaternary Science Reviews*, *140*, 142–162. https://doi.org/10.1016/j.quascirev.2016.03.027

Smik, L., & Belt, S. T. (2017). Distributions of the Arctic sea ice biomarker proxy IP$_{25}$ and two phytoplanktonic biomarkers in surface sediments from West Svalbard. *Organic Geochemistry*, *105*, 39–41. https://doi.org/10.1016/j.orggeochem.2017.01.005

Smik, L., Cabedo-Sanz, P., & Belt, S. T. (2016). Semi-quantitative estimates of paleo Arctic sea ice concentration based on source-specific highly branched isoprenoid alkenes: A further development of the PIP25 index. *Organic Geochemistry*, *92*, 63–69. https://doi.org/10.1016/j.orggeochem.2015.12.007

Spielhagen, R. F., Baumann, K.-H., Erlenkeuser, H., Nowaczyk, N. R., Nørgaard-Pedersen, N., Vogt, C., & Weiel, D. (2004). Arctic Ocean deep-sea record of northern Eurasian ice sheet history. *Quaternary Science Reviews*, *23*(11–13), 1455–1483. https://doi.org/10.1016/j.quascirev.2003.12.015

Stein, R. (2008). *Arctic Ocean sediments: processes, proxies, and paleoenvironment*. Amsterdam: Elsevier.

Stein, R. (2015). The Expedition PS87 of the Research Vessel POLARSTERN to the Arctic Ocean in 2014. Berichte zur Polar- und Meeresforschung.

Stein, R. (Ed.) (2016). The Expedition PS93.1 of the Research Vessel POLARSTERN to the Greenland Sea and the Fram Strait in 2015. Berichte zur Polar- und Meeresforschung 2016.

Stein, R., & Fahl, K. (2013). Biomarker proxy IP25 shows potential for studying entire Quaternary Arctic sea-ice history. *Organic Geochemistry*, *55*, 98–102. https://doi.org/10.1016/j.orggeochem.2012.11.005

Stein, R., Fahl, K., Gierz, P., Niessen, F., & Lohmann, G. (2017). Arctic Ocean sea ice cover during the penultimate glacial and the last interglacial. *Nature Communications*, *8*, 373, 45571. https://doi.org/10.1038/s41467-017-00552-1

Stein, R., Fahl, K., & Müller, J. (2012). Proxy reconstruction of Cenozoic Arctic Ocean sea-ice history—From IRD to IP25. *Polarforschung*, *82*(1), 37–71.

Stein, R., Fahl, K., Schreck, M., Knorr, G., Niessen, F., Forwick, M., & Lohmann, G. (2016). Evidence for ice-free summers in the late Miocene central Arctic Ocean. *Nature Communications*, *7*, 11148. https://doi.org/10.1038/ncomms11148

Stein, R., Grobe, H., & Wahsner, M. (1994). Organic carbon, carbonate, and clay mineral distributions in eastern central Arctic Ocean surface sediments. *Marine Geology*, *119*(3–4), 269–285. https://doi.org/10.1016/0025-3227(94)90185-6

Stein, R., & Macdonald, R. W. (2004). *The organic carbon cycle in the Arctic Ocean*. Berlin Heidelberg: Springer. https://doi.org/10.1007/978-3-642-18912-8

Stoecker, D. K., Gustafson, D. E., Black, M. M., & Baier, C. T. (1998). Population dynamics of microalgae in the upper land-fast sea ice at a snow-free location. *Journal of Phycology*, *34*(1), 60–69. https://doi.org/10.1046/j.1529-8817.1998.340060.x

Stoynova, V., Shanahan, T. M., Hughen, K. A., & de Vernal, A. (2013). Insights into circum-Arctic sea ice variability from molecular geochemistry. *Quaternary Science Reviews*, *79*, 63–73. https://doi.org/10.1016/j.quascirev.2012.10.006

Stroeve, J., Holland, M. M., Meier, W., Scambos, T., & Serreze, M. (2007). Arctic sea ice decline: Faster than forecast. *Geophysical Research Letters*, *34*, L09501. https://doi.org/10.1029/2007GL029703

Stroeve, J., & Notz, D. (2018). Changing state of Arctic sea ice across all seasons. *Environmental Research Letters*, *13*, 103001. https://doi.org/10.1088/1748-9326/aade56

Stroeve, J. C., Serreze, M. C., Holland, M. M., Kay, J. E., Malanik, J., & Barrett, A. P. (2012). The Arctic's rapidly shrinking sea ice cover: A research synthesis. *Climatic Change*, *110*(3–4), 1005–1027. https://doi.org/10.1007/s10584-011-0101-1

Summons, R. E., Capon, R. J., Stranger, C., & Barrow, R. A. (1993). The structure of a new C$_{25}$ isoprenoid alkene biomarker from diatomaceous microbial communities. *Australian Journal of Chemistry.*, *46*(6), 907–915. https://doi.org/10.1071/CH9930907

Swart, N. (2017). Natural causes of Arctic sea-ice loss. *Nature Climate Change*, *7*(4), 239. Retrieved from–241. https://doi.org/10.1038/nclimate3254

Swart, N. C., Fyfe, J. C., Hawkins, E., Kay, J. E., & Jahn, A. (2005). Influence of internal variability on Arctic sea-ice trends. *Nature Climate Change*, *5*(2), 86–89.

Tang, C. C. L., Ross, C. K., Yao, T., Petrie, B., DeTracey, B. M., & Dunlap, E. (2004). The circulation, water masses and sea-ice of Baffin Bay. *Progress in Oceanography*, *63*(4), 183–228. https://doi.org/10.1016/j.pocean.2004.09.005

ter Braak, C. J. F., & Šmilauer, P. (2002). *CANOCO Reference Manual and CanoDraw for Windows user's guide: Software for Canonical Community Ordination (Version 4.5), Section on Permutation Methods*. Ithaca, New York: Microcomputer Power.

Thomas, D. N. (2012). Sea ice. In M. E. Bell (Ed.), *Life in extremes: Environments, organisms and strategies for survival* (pp. 62–80). Oxford, UK: CABI Publishing. https://doi.org/10.1079/9781845938147.0062

Thomas, D. N., & Dieckmann, G. S. (2010). *Sea Ice*. Oxford: Blackwell Publishing.

Uenzelmann-Neben, G. (2009). Cruise Report RV MARIA S. MERIAN Cruise MSM12-2 Reykjavik - Reykjavik. https://doi.org/10.2312/cr_msm12_2

Vare, L. L., Massé, G., Gregory, T. R., Smart, C. W., & Belt, S. T. (2009). Sea ice variations in the central Canadian Arctic Archipelago during the Holocene. *Quaternary Science Reviews*, *28*(13–14), 1354–1366. https://doi.org/10.1016/j.quascirev.2009.01.013

Vogt, C., Knies, J., Spielhagen, R. F., & Stein, R. (2001). Detailed mineralogical evidence for two nearly identical glacial/deglacial cycles and Atlantic water advection to the Arctic Ocean during the last 90,000 years. *Global and Planetary Change*, *31*(1–4), 23–44. https://doi.org/10.1016/S0921-8181(01)00111-4

Volkman, J. K. (1986). A review of sterol markers for marine and terrigenous organic matter. *Organic Geochemistry*, *9*(2), 83–99. https://doi.org/10.1016/0146-6380(86)90089-6

Volkman, J. K., Barrett, S. M., Dunstan, G. A., & Jeffrey, S. W. (1993). Geochemical significance of the occurrence of dinosterol and other 4-methyl sterols in a marine diatom. *Organic Geochemistry.*, *20*(1), 7–15. https://doi.org/10.1016/0146-6380(93)90076-N

Volkman, J. K., Farrington, J., Gagosian, R. B., & Wakeham, S. G. (1983). Lipid composition of coastal marine sediments from the Peru upwelling region. In *Advances in organic geochemistry* (Vol. 1981, pp. 228–240). Chichester: Wiley. Retrieved from http://ci.nii.ac.jp/naid/80001914941/

Vorrath, M. E., Müller, J., Esper, O., Mollenhauer, G., Haas, C., Schefuß, E., & Fahl, K. (2019). Highly branched isoprenoids for Southern Ocean sea ice reconstructions: A pilot study from the Western Antarctic Peninsula. *Biogeosciences*, *16*(15), 2961–2981. https://doi.org/10.5194/bg-16-2961-2019

Walsh, J. J. (1989). Arctic carbon sinks: Present and future. *Global Biogeochemical Cycles*, *3*(4), 393–411. https://doi.org/10.1029/GB003i004p00393

Wassmann, P., Duarte, C. M., Agustí, S., & Sejr, M. K. (2011). Footprints of climate change in the Arctic marine ecosystem. *Global Change Biology*, *17*(2), 1235–1249. https://doi.org/10.1111/j.1365-2486.2010.02311.x

Wegner Koch, C., Cooper, L. W., Lalande, C., Brown, T. A., Frey, K. E., & Grebmeier, J. M. (2020). Seasonal and latitudinal variations in sea ice algae deposition in the Northern Bering and Chukchi Seas determined by algal biomarkers. *PLoS ONE*, *15*(4), e0231178. https://doi.org/10.1371/journal.pone.0231178

Werner, K., Spielhagen, R. F., Bauch, D., Hass, H. C., Kandiano, E., & Zamelczyk, K. (2011). Atlantic Water advection to the eastern Fram Strait—Multiproxy evidence for late Holocene variability. *Palaeogeography, Palaeoclimatology, Palaeoecology*, *308*(3–4), 264–276. https://doi.org/10.1016/j.palaeo.2011.05.030

Whitney, F. A., Crawford, W. R., & Harrison, P. J. (2005). Physical processes that enhance nutrient transport and primary productivity in the coastal and open ocean of the subarctic NE Pacific. *Deep-Sea Research II*, *53*, 681–706.

WOA13; World Ocean Atlas (2013). https://www.nodc.noaa.gov/OC5/woa13/woa13data.html

Wohlfahrt, J., Harrison, S. P., & Braconnot, P. (2004). Synergistic feedbacks between ocean and vegetation on mid- and high-latitude climates during the mid-Holocene. *Climate Dynamics*, *22*(2–3), 223–238. https://doi.org/10.1007/s00382-003-0379-4

Wollenburg, E., Kuhnt, W., & Mackensen, A. (2001). Changes in Arctic Ocean paleoproductivity and hydrography summer East Greenland Current—Passage of outflowing Arctic. *Paleoceanography*, *16*(1), 65–77. https://doi.org/10.1029/1999PA000454

Wollenburg, J. E., Knies, J., & Mackensen, A. (2004). High-resolution paleoproductivity fluctuations during the past 24 kyr as indicated by benthic foraminifera in the marginal Arctic Ocean. *Palaeogeography, Palaeoclimatology, Palaeoecology*, *204*(3–4), 209–238. https://doi.org/10.1016/S0031-0182(03)00726-0

Xiao, X., Fahl, K., Müller, J., & Stein, R. (2015). Sea-ice distribution in the modern Arctic Ocean: Biomarker records from trans-Arctic Ocean surface sediments. *Geochimica et Cosmochimica Acta*, *155*, 16–29. https://doi.org/10.1016/j.gca.2015.01.029

Xiao, X., Fahl, K., & Stein, R. (2013). Biomarker distributions in surface sediments from the Kara and Laptev seas (Arctic Ocean): Indicators for organic-carbon sources and sea-ice coverage. *Quaternary Science Reviews*, *79*, 40–52. https://doi.org/10.1016/j.quascirev.2012.11.028

Yruela, I., Barbe, A., & Grimalt, J. O. (1990). Determination of double bond position and geometry in linear and highly branched hydrocarbons and fatty acids from gas chromatography-mass spectrometry of epoxides and diols generated by stereospecific resin hydration. *Journal of Chromatographic Science*, *28*(8), 421–427. https://doi.org/10.1093/chromsci/28.8.421

Zamani, B., Krumpen, T., Smedsrud, L. H., & Gerdes, R. (2019). Fram Strait sea ice export affected by thinning: Comparing high-resolution simulations and observations. *Climate Dynamics*, *53*(5–6), 3257–3270. https://doi.org/10.1007/s00382-019-04699-z